École polytechnique de Louvain

Impact of Battery Storage on Congestion Management in the CWE Region

Author: **Reza Javadian**
Supervisor: **Quentin Lété**
Readers: **Emmanuel De Jaeger, Gilles Ooms**
Academic year 2025–2026
Master [120] in Electro-mechanical Engineering

Abstract

The rapid expansion of variable renewable generation across Central Western Europe (CWE) is intensifying intra-zonal transmission congestion and the associated re-dispatch costs borne by transmission system operators (TSO's). Battery energy storage systems (BESS) are increasingly deployed as a flexibility resource, yet their net impact on physical network congestion remains poorly understood. This thesis investigates whether price-arbitrage BESS deployment in Belgium increases or decreases intra-zonal re-dispatch costs, and how this effect evolves as installed capacity scales from 800 MW to 6,000 MW.

A two-stage simulation framework is developed, combining a flow-based zonal pricing (ZPFB) model with a nodal DC optimal power flow (DCOPF) re-dispatch model applied to the full CWE network. Two generation datasets are considered: a 2018 thermal-dominated baseline and an updated 2025 dataset reflecting Belgium's partial nuclear phase-out and the significant expansion of solar and wind capacity across the region. Two re-dispatch methods define the range of options for cross-border coordination among TSO's.

Results show that battery deployment consistently increases Belgian re-dispatch costs under both methods and both datasets, as price-arbitrage dispatch creates injection patterns that aggravate existing corridor overloads. However, the net economic balance (zonal generation cost savings minus the incremental re-dispatch cost) remains robustly positive and grows with capacity, reaching 35.1 M€/year in 2018 and 68.2 M€/year in 2025 at 6,000 MW. The 2025 high-renewable context amplifies both the arbitrage value, driven by the solar duck curve, and the re-dispatch impact, while inverting the sign of Belgium's cost allocation under full EU-wide TSO coordination. These findings suggest that the economic benefits of large-scale Belgian BESS will strengthen with the energy transition, but that realising the full benefit requires closer alignment between battery dispatch and transmission system operation.

Acknowledgment

I would like to begin by thanking my supervisor, Quentin Lété, who proposed this topic and agreed to take me on despite my background being in energy engineering rather than optimisation. His patience in bridging that gap, his availability for weekly meetings throughout the year, and his willingness to engage with every question I brought to him made this work possible. The course in Quantitative Energy Economics that he taught also gave me the analytical foundations without which I could not have started.

I am equally grateful to Emmanuel De Jaeger, whose power systems courses and seminar series opened a window onto the Belgian and European electricity sector long before I began writing. It was Professor De Jaeger who first suggested I contact Quentin Lété, following the report they had co-authored, and I am glad he did. I also thank him for agreeing to serve on the jury for this thesis.

I would also like to thank Louis Magein of Elia, whose presentation of the AdeqFlex 2025 study introduced me to the scenario framework that became central to this thesis, Tobias Löwenthal and Natan Ghyoot, who read much of this manuscript and whose comments were more helpful than they probably realize, and my sister, Sara Javadian, who was writing her own thesis at the same time and made the whole experience considerably less lonely.

Parts of this thesis were drafted with the assistance of AI-based writing tools. Claude [1] was used to support writing, proofreading, and literature search, and DeepL [2] was used for translation assistance.

Contents

1 Introduction

1.1 Context and Research Question

The decarbonisation of electricity systems is driving a structural transformation of the European generation mix. As wind and solar capacity continues to expand to meet climate objectives, the share of renewable energy in electricity generation across Europe is projected to exceed 70% by 2036, up from 47% in 2024. For Belgium specifically, this share is projected to reach between 44% and 54% of total electricity demand by 2036, depending on the scenario [3]. Unlike dispatchable thermal units, these sources cannot be scheduled on demand: their output depends on meteorological conditions rather than on system needs, creating a structural mismatch between supply and demand that must be actively managed.

Battery energy storage systems (BESS) are increasingly deployed as one of the primary responses to this challenge. By storing electrical energy during periods of surplus and releasing it during periods of scarcity, they provide temporal flexibility, reduce wholesale price volatility, and displace costly peaking generation [4]. In Belgium, installed BESS capacity reached approximately 0.8 GW by 2025 and is projected under Elia's adequacy and flexibility study to grow to between 3.9 and 6.0 GW by 2035, depending on the deployment scenario considered [3].

The costs of managing physical network constraints are substantial and growing. Across Europe, annual re-dispatch expenditures have risen sharply as renewable penetration has increased, reaching several billion euros in Germany [5] and increasing steadily in Belgium as the generation mix becomes more geographically dispersed and variable [6]. Elia bears these costs directly and recovers them through network tariffs borne by end consumers. As offshore wind capacity continues to scale up and nuclear generation is restructured, the frequency and severity of intra-zonal overloads on specific Belgian transmission corridors is projected to increase further.

Belgium occupies a structurally interesting position in this transition. Historically, its generation mix has been dominated by large nuclear units concentrated at a small number of sites, which produced spatially stable and predictable power flows on the high-voltage network. The ongoing restructuring of this mix (nuclear output being progressively replaced by offshore wind turbines concentrated along the North Sea coast, increased cross-border imports, and emerging grid-scale battery capacity) is shifting power injection patterns in ways that load new internal corridors and relieve others. Batteries, in particular, introduce highly dynamic, price-driven charge and discharge cycles that interact with this evolving injection geography in ways that are not yet well understood [3].

While the economic benefits of battery arbitrage are well understood at the market level, their impact on the physical transmission network is considerably less clear. A battery is not just a financial instrument for price smoothing: it is a physical asset connected at a specific node of the network, and its charge and discharge decisions impose real power flows on real transmission lines. These flows may decrease existing congestion in some operating conditions, but can also worsen it in others.

The central question of this thesis is therefore: *Does the deployment of battery storage in Belgium increase or decrease intra-zonal transmission congestion, and how does this effect evolve as battery capacity scales up?*

1.2 Related Work

The interaction between electricity storage and transmission networks has attracted growing attention in the literature, particularly as BESS deployment has accelerated across Europe.

At the market level, the benefit of battery storage has been widely studied through the lens of price arbitrage [7, 8]. These studies consistently show that batteries improve market efficiency by reducing intraday price differences, and that their benefit grows with price volatility — a pattern that becomes stronger as renewable penetration increases [9]. However, these analyses assume a copper-plate network and therefore cannot capture any physical grid effects.

At the physical network level, the relationship between storage and congestion is less straightforward. A battery charging during off-peak periods can absorb excess local generation and reduce line loading, but a battery discharging at a single node during peak demand may equally worsen existing overloads. The net effect depends on where the battery is located, the prevailing generation pattern, and which network constraints are binding at each hour. Storage operated purely for price arbitrage does not systematically provide grid relief: its effect on redispatch depends on coincidental alignment between market and network conditions at each hour [10].

In the European context, a separate strand of literature has examined the gap between the zonal day-ahead market clearing and the subsequent physical re-dispatch carried out by transmission system operators [11]. Under flow-based market coupling (FBMC), cross-border constraints are enforced at the market stage, but intra-zonal network feasibility is not. The system operator must therefore correct physically infeasible schedules through re-dispatch actions at a cost — a process that has grown significantly across Europe as generation patterns have become more variable under the energy transition [5, 6]. In Belgium, Elia regularly redispatches generators to resolve overloads on specific internal corridors, and the cost of these interventions is ultimately passed on to end consumers.

Despite this body of work, the specific impact of BESS on intra-zonal re-dispatch costs in the Belgian context under FBMC has not been systematically studied across a range of deployment scenarios. Existing studies either focus on isolated network segments, use simplified market representations, or address battery arbitrage and regulatory aspects of BESS-grid interaction without isolating the congestion channel [12]. This thesis addresses that gap through an explicit two-stage simulation framework (zonal pricing followed by nodal re-dispatch) applied to the full CWE network under both a 2018 baseline and a 2025 generation mix.

1.3 Modelling Approach

The modelling framework decomposes the problem into two sequential stages, each corresponding to a distinct operational stage of the European electricity system.

The first stage is a **zonal pricing model** based on flow-based market coupling [11], which represents how the day-ahead electricity market clears across the CWE region. Each country constitutes a single bidding zone: within a zone, electricity is assumed to flow freely between any two points (the copper-plate assumption), while cross-zonal exchanges are constrained by power transfer distribution factor (PTDF) matrices computed from the physical network. This corresponds precisely to how European day-ahead markets operate today. The model determines the least-cost generation dispatch and the associated zonal prices for each hour of the year.

The second stage is a **nodal re-dispatch model**, which checks whether the dispatch produced by the zonal market is physically feasible on the full high-voltage network, including all intra-zonal transmission lines. When thermal limits are violated, the model computes the least-cost corrective adjustment: some generators reduce output (down-regulation) and others increase theirs (up-regulation), at a cost borne by the system operator. This stage is where physical line limits actually bind and where the impact of batteries on congestion can be properly measured.

Two variants of the re-dispatch model are compared. Method A is an unconstrained CWE-wide DC optimal power flow, which serves as an efficiency benchmark: all generators across the six countries can be redispatched freely, and the optimal solution provides a lower bound on re-dispatch cost. Method B adds a single constraint that fixes the Belgian zone's net import/export position to its day-ahead market value, so that only intra-zonal Belgian re-dispatch is permitted — reflecting standard European practice, in which inter-zonal market allocations are preserved at the re-dispatch stage. The two annual re-dispatch cost series, C^A and C^B, are reported separately across all battery scenarios throughout this thesis.

A key modelling assumption is the treatment of battery storage at the re-dispatch stage. This thesis adopts the working hypothesis that batteries are not available for re-dispatch. This reflects the current absence of a well-established mechanism for pricing battery opportunity costs within standard pay-as-bid re-dispatch auctions, and is consistent with observed TSO practice in the CWE region. The working hypothesis of this thesis is therefore that **batteries are not available for re-dispatch**: once the zonal market has determined the battery's charge-discharge schedule, that schedule is treated as fixed at the re-dispatch stage. The TSO adjusts only conventional generators. This assumption has an important implication: the battery's dispatch profile, optimised for price arbitrage without any knowledge of intra-zonal network constraints, creates power flows on the physical network that may relieve or worsen congestion. Whether it does one or the other is precisely the question this thesis addresses. This assumption will be handled in Section 2.2 and Section 2.3.

1.4 Case Study and Scope

The analysis is applied to the Central Western Europe region, which covers Belgium, France, Germany, Luxembourg, the Netherlands, and Austria. This perimeter is chosen because Belgian transmission flows are tightly coupled with those of its neighbours: cross-border imports and exports regularly load Belgian internal lines, and an assessment of Belgian congestion that ignores the broader regional power balance would be incomplete.

Two generation datasets are considered to capture the effect of the ongoing energy transition. The first corresponds to the 2018 system, which serves as a validated baseline with a well-documented generation mix. The second is an updated dataset calibrated to represent the 2025 power system, reflecting Belgium's partial nuclear phase-out, significant additions of offshore wind capacity, and the continued decline of coal-fired generation across the CWE region. Comparing results across the two datasets isolates how the energy transition alters the battery-congestion relationship.

Battery storage is modelled as a price-taking agent located within the Belgian bidding zone, with capacity levels drawn from Elia's adequacy and flexibility scenarios [3]. Five scenarios are considered, ranging from zero storage to 6 GW. The aim of this work is not to determine the optimal battery siting strategy, nor to prescribe a transmission investment plan. What it provides is a concrete and reproducible measure of how intra-zonal re-dispatch costs evolve as battery deployment scales up.

The rest of this thesis is organised as follows. Section 2 presents the mathematical formulation of both models and the integration of battery storage. Section 3 describes the datasets, presents the simulation results for both generation mixes, and discusses the key findings. Section 4 addresses the limitations of the approach and possible extensions. Section 5 concludes.

2 Mathematical model

2.1 Zonal Pricing

The first step of the simulation pipeline is to model how electricity is priced and dispatched across the market area. This step is called zonal pricing, and it corresponds to how European day-ahead electricity markets operate in practice. Understanding it is essential before discussing re-dispatch or the role of batteries, because it is this market stage that determines which generators run, at what output level, and what price consumers pay in each zone.

This section explains the concept behind zonal pricing, presents the mathematical optimisation model, and describes how it is implemented.

2.1.1 Market Design and the Copper-Plate Assumption

In a zonal electricity market, the market area is partitioned into a set of bidding zones. Within each zone, it is assumed that electricity can flow freely between any generator and any consumer without internal network constraints. This is the **copper-plate assumption**: the transmission grid inside each zone is treated as a perfect conductor with unlimited capacity for internal exchanges. As a result, a single electricity price prevails across the entire zone at each period, regardless of the physical location of generators and consumers.

Between zones, power can be exchanged, but inter-zonal flows are constrained by the physical capacity of the transmission infrastructure connecting them. The traditional approach represents these limits through a single aggregate number per zone pair, called the **Available Transfer Capacity** (ATC): the maximum net flow allowed between two zones. The ATC approach does not reflect how power actually behaves in a network: an exchange between two zones does not travel exclusively along the direct interconnector. Because of Kirchhoff's laws, part of that flow redistributes through alternative paths in the network. These are called loop flows, and they load lines that do not directly connect the two trading zones.

This thesis instead uses **flow-based market coupling** (FBMC), which constrains the physical flow on each individual critical branch using a DC power flow model. Rather than one limit per border, there is a separate limit for each critical branch in the network. This is the approach adopted in practice by several European market coupling regions, replacing the older ATC methodology [13].

Even with this more detailed network representation, the model still treats each zone as a single node: all internal transmission constraints within a zone are ignored. This is the copper-plate assumption, and it is precisely the reason why a re-dispatch step is needed after the market clears.

2.1.2 Mathematical Model

General Formulation

The flow-based zonal pricing model is presented in Papavasiliou [11] (Section 5.3) as a social welfare maximisation problem, denoted **(ZPFB)**:

$$\max_{p,\,d,\,r,\,f} \quad \sum_{\ell \in \mathcal{L}} \int_0^{d_\ell} \mathrm{MB}_\ell(x)\,\mathrm{d}x \;-\; \sum_{g \in \mathcal{G}} \int_0^{p_g} \mathrm{MC}_g(x)\,\mathrm{d}x \qquad \text{(ZPFB)}$$

where $d_\ell \geq 0$ is the consumption of load ℓ (MW) and $p_g \geq 0$ is the production of conventional generator g (MW). $\mathrm{MB}_\ell(x)$ and $\mathrm{MC}_g(x)$ are the marginal benefit of the consumers at load l and the marginal cost of the generator g respectively.

This equation is subject to several constraints, for each zone $z \in \mathcal{Z}$:

$$(\rho_z): \quad r_z = \sum_{g \in \mathcal{G}_z} p_g - \sum_{\ell \in \mathcal{L}_z} d_\ell \tag{1}$$

$$f_k = \sum_{z \in \mathcal{Z}} \mathrm{PTDF}_{kz} \cdot r_z, \quad k \in \mathcal{CB} \tag{2}$$

$$|f_k| \leq \mathrm{RAM}_k, \quad k \in \mathcal{CB} \tag{3}$$

$$\sum_{z \in \mathcal{Z}} r_z = 0 \tag{4}$$

$$p_g \geq 0, \quad d_\ell \geq 0 \tag{5}$$

Here $\mathcal{Z}$ is the set of bidding zones, $\mathcal{G}$ the set of dispatchable generators with $\mathcal{G}_z \subseteq \mathcal{G}$ the subset located in zone z, and $\mathcal{L}$ the set of loads with $\mathcal{L}_z \subseteq \mathcal{L}$ the loads of zone z. The set $\mathcal{CB}$ contains the cross-border lines: the physical network elements for which flow constraints are enforced.

The three key decision variables are p_g, d_ℓ and $r_z \in \mathbb{R}$. r_z is the net position of zone z (MW), which corresponds either to an export for the region when $r_z > 0$, or to an import when $r_z < 0$.

The flow f_k in (2) is not an independent decision variable: it is derived from the net positions via the zone-to-line sensitivity coefficients PTDF_{kz}. The **Power Transfer Distribution Factor** matrix $\mathrm{PTDF} \in \mathbb{R}^{k \times z}$ measures the fraction of a unit power injection in zone z that flows through line k. Its computation is explained later in this section.

Constraint (1) defines the net position of each zone as the difference between total generation and total consumption within that zone. Its dual variable ρ_z is the zonal price, discussed in detail below.

Constraint (3) imposes a hard upper bound on the physical flow on each cross-border line, where RAM_k (Remaining Available Margin) is the capacity available for market exchanges.

Constraint (4) is the global market clearing condition: the sum of all net positions must be zero, ensuring total generation equals total consumption across the region.

From Welfare Maximisation to Cost Minimisation

In this thesis, electricity demand is treated as **perfectly inelastic**: each zone must consume a fixed quantity at each period, regardless of price. Since consumption is fixed, the benefit terms in the objective (ZPFB) are constant with respect to the dispatch decision and can be dropped. Maximising social welfare is then equivalent to minimising total generation cost [11]:

$$\min_{p} \quad \sum_{g \in \mathcal{G}} c_g \cdot p_g \tag{6}$$

where c_g (€/MWh) is the marginal cost of generator g, considered constant.

Adaptations to the implemented model

Three adaptations are required to move from the general model (ZPFB)–(5) to the formulation actually implemented.

(i) Net demand: Not all generation units are dispatchable. Renewable sources (wind, solar, run-of-river hydro) and other fixed-schedule units produce power determined by physical conditions rather than by market optimisation. Such generation is treated as **must-run**: it reduces the demand that dispatchable generators must cover. Let $R_z(t)$ denote the aggregate must-run output in zone z at period t. The net demand is defined as:

$$D_z^{\mathrm{net}}(t) = D_z(t) - R_z(t) \tag{7}$$

where $D_z(t)$ is gross load (MW). The net demand $D_z^{\text{net}}(t)$ is the quantity that dispatchable generators must collectively cover. It may be negative in hours of high renewable output, signalling a surplus that must be exported or curtailed.

(ii) Zone-to-line PTDFs via Generation Shift Keys: Constraint (2) requires the zone-to-line sensitivity coefficients PTDF_{kz}, measuring how a unit increase in the net position r_z of zone z flows on cross-border line k. The starting point is the node-to-line PTDF matrix: its entry PTDF_{kb} gives the fraction of a unit injection at bus b (with simultaneous withdrawal at the reference bus) that flows on line k. It is computed from the bus susceptance matrix $B_{\text{bus}} \in \mathbb{R}^{|\mathcal{N}|\times|\mathcal{N}|}$:

$$(B_{\text{bus}})_{nm} = \begin{cases} \sum\limits_{k:\, n\in k} b_k & \text{if } n = m \\ -b_{nm} & \text{if line } (n,m) \text{ exists} \\ 0 & \text{otherwise} \end{cases} \tag{8}$$

where $b_k = 1/X_k$ is the susceptance of line k, and X_k (Ω) is the series reactance of line k. Then we fix a reference (slack) bus and remove its corresponding row and column from the susceptance marix, to get the reduced matrix B_{red}. The node-to-line PTDF entry is then:

$$\text{PTDF}_{kb} \;=\; b_k \left(\left(B_{\text{red}}^{-1}\right)_{\text{from}(k),\, b} \;-\; \left(B_{\text{red}}^{-1}\right)_{\text{to}(k),\, b} \right) \tag{9}$$

for all non-slack buses b, with $\text{PTDF}_{k,\,\text{slack}} = 0$ by convention. These coefficients depend only on network topology and line parameters and are computed once before the simulation loop.

To obtain the zone-to-line PTDF_{kz}, the node-level sensitivities are aggregated across all buses in zone z using Generation Shift Keys (GSK). The $\text{GSK}_z[g]$ of generator g in zone z represents the fraction of a unit change in the net export of zone z that is injected at bus(g). Following the standard CWE flow-based methodology [13],a capacity-weighted GSK is used:

$$\text{GSK}_z[g] \;=\; \frac{P_g^{\max}}{\sum\limits_{g'\in\mathcal{G}_z} P_{g'}^{\max}} \tag{10}$$

The zone-to-line PTDF is then the GSK-weighted average of node-level sensitivities:

$$\text{PTDF}_{kz} \;=\; \sum_{g\in\mathcal{G}_z} \text{GSK}_z[g] \cdot \text{PTDF}_{k,\,\text{bus}(g)} \tag{11}$$

The physical flow on critical branch k is therefore:

$$f_k \;=\; \sum_{z\in\mathcal{Z}} \text{PTDF}_{kz} \cdot r_z \tag{12}$$

which is exactly expression (2). This reduces the sensitivity information from the full nodal PTDF matrix (one entry per line per bus) to a compact matrix of size $|\mathcal{CB}| \times |\mathcal{Z}|$, directly exploitable in the optimisation model.

(iii) Feasibility and the Value of Lost Load: In a flow-based model with hard constraints (3), feasibility of the market equilibrium is not guaranteed for every combination of demand and renewable output. When large net-position imbalances arise, the implied physical flows on certain cross-border lines may exceed their capacity bounds regardless of how generation is redispatched within the zonal model. This is not a modelling artefact: it reflects that zonal pricing, by design, cannot fully resolve network congestion.

Rather than relaxing the constraints with an ad-hoc penalty, which would distort the dual variables and corrupt the zonal prices, this thesis follows the standard European market convention and introduces a **Value of Lost Load** (VOLL) [13]. Two complementary adjustment variables are added:

- $\text{ls}_z(t) \in [0,\, D_z(t)]$: load shedding in zone z at period t (MW). Activates when the network cannot import enough power to meet demand; its cost in the objective is VOLL €/MWh. By complementary slackness, $\rho_z(t) = \text{VOLL}$ whenever $\text{ls}_z(t) > 0$.

- $\mathrm{rc}_z(t) \in [0,\, R_z(t)]$: renewable curtailment in zone z at period t (MW). Activates when must-run output exceeds demand and the surplus cannot be exported due to binding flow constraints; its cost is zero. By complementary slackness, $\rho_z(t) = 0$ whenever $\mathrm{rc}_z(t) > 0$.

Together, these two variables guarantee that the optimisation problem always admits a feasible solution, while preserving the economic meaning of the dual variables: zonal prices are bounded in [0, VOLL] at all times.

Implemented Optimisation Problem

Combining all the above, the full implemented model is:

$$\min_{p,\, r,\, \mathrm{ls},\, \mathrm{rc}} \quad \sum_{g\in\mathcal{G}} \sum_{t=1}^{T} c_g \cdot p_g(t) \;+\; \mathrm{VOLL} \cdot \sum_{z\in\mathcal{Z}} \sum_{t=1}^{T} \mathrm{ls}_z(t) \tag{ZPFB*}$$

s. t., for all $z \in \mathcal{Z}$ and $t = 1, \ldots, T$:

$$(\rho_z(t)): \quad \sum_{g\in\mathcal{G}_z} p_g(t) + \mathrm{ls}_z(t) - \mathrm{rc}_z(t) - r_z(t) = D_z^{\mathrm{net}}(t) \tag{13}$$

$$\sum_{z\in\mathcal{Z}} r_z(t) = 0 \tag{14}$$

$$\sum_{z\in\mathcal{Z}} \mathrm{PTDF}_{kz} \cdot r_z(t) \;\le\; \mathrm{TC}_k^{+}, \quad k \in \mathcal{CB} \tag{15}$$

$$\sum_{z\in\mathcal{Z}} \mathrm{PTDF}_{kz} \cdot r_z(t) \;\ge\; -\mathrm{TC}_k^{-}, \quad k \in \mathcal{CB} \tag{16}$$

$$0 \;\le\; p_g(t) \;\le\; P_g^{\max} \tag{17}$$

$$0 \;\le\; \mathrm{ls}_z(t) \;\le\; D_z(t) \tag{18}$$

$$0 \;\le\; \mathrm{rc}_z(t) \;\le\; R_z(t) \tag{19}$$

Constraint (13) is the zone energy balance: it defines the net position $r_z(t)$ as effective supply minus net demand. Its dual $\rho_z(t)$ is the zonal price. Constraint (14) ensures global market clearing. Constraints (15)–(16) are the hard flow limits on cross-border lines. Constraints (17)–(19) are variable bounds. When a battery is present in zone $\mathcal{Z}$, the balance constraint (13) for that zone is extended to include the battery net injection $(d^{\mathrm{bat}}(t) - c^{\mathrm{bat}}(t))$. The full battery model is described in Section 2.3.

Zonal Prices as Dual Variables

The main output of model (ZPFB*) is the zonal price $\rho_z(t)$: the dual variable of the energy balance constraint (13). At optimality, it equals the marginal cost of the last unit dispatched to cover demand in zone z at period t. Low-cost units (e.g. nuclear, run-of-river hydro) are dispatched first; the price is set by the most expensive unit needed to meet net demand.

The VOLL and renewable-curtailment variables impose tight bounds by complementary slackness:

$$0 \;\le\; \rho_z(t) \;\le\; \mathrm{VOLL} \qquad \forall\, z \in \mathcal{Z},\; t = 1, \ldots, T.$$

When two adjacent zones are not separated by a congested cross-border line, their prices equalize. A price difference between zones therefore signals binding congestion on at least one cross-border line [11]: the cheaper zone cannot export enough to equate prices with its neighbours.

Implementation

The model is implemented in Julia [14] using the JuMP modelling framework [15] and solved with the HiGHS linear programming solver [16]. All T periods of the simulation horizon are formulated as a single multi-period linear programme. This is necessary when a battery is present, because the state-of-charge dynamics couple consecutive periods and the problem cannot be decomposed into independent single-period instances.

2.1.3 Limitations of Zonal Pricing

The zonal pricing model provides the dispatch schedule and zonal prices, but rests on the copper-plate assumption: within each zone, the grid is treated as having unlimited internal capacity. The model decides that a generator at one location should produce p_g^* MW while another is idle, and implicitly assumes the resulting flows are feasible on the internal transmission network. This is often not the case.

In practice, concentrated generation (e.g. offshore wind in one region) combined with consumption elsewhere regularly exceeds the capacity of internal lines. The zonal model cannot detect this problem because it treats the entire zone as a single node. Congestion originating from internal exchange is invisible to the market.

This is where re-dispatch intervenes. Once the market has cleared, the transmission system operator (TSO) checks whether the scheduled dispatch is physically feasible on the actual network. When lines are overloaded, some generators are instructed to reduce their output (down-regulation) and others to increase it (up-regulation), until all thermal limits are satisfied.

Re-dispatch comes at a cost: generators that are curtailed must be compensated, and those that ramp up must be paid. This re-dispatch cost is the central metric of this thesis. It captures everything that the zonal pricing model, with its copper-plate assumption, fails to see. When batteries are introduced, the key question becomes whether their presence increases or reduces this cost, and by how much.

2.2 Redispatch

The zonal pricing model determines, for each period, which conventional generators should run and at what output level, treating each bidding zone as a copper plate with unlimited internal transmission capacity. In reality, the power injected at each bus must flow through physical transmission lines, each with a finite thermal limit. A dispatch schedule that is market-feasible at the zonal level may therefore produce line overloads on the actual network. Re-dispatch corrects this: once the zonal market has cleared, the system operator identifies overloads and adjusts individual generator outputs to restore physical feasibility.

This section presents the general re-dispatch model, describes how it is adapted to the dataset at hand, and introduces the two implementation methods whose costs are compared throughout the thesis.

2.2.1 From Zonal Market to Physical Network

The zonal pricing model produces, for each period t, a dispatch schedule $p_g^*(t)$ for every generator $g \in \mathcal{G}$ and a set of inter-zonal flows. This schedule is market-feasible: it satisfies energy balance in each zone and respects the inter-zonal PTDF constraints used in the zonal clearing. It is not, however, guaranteed to be network-feasible: mapping each generator to its physical bus and propagating the injections through the full transmission network may overload individual lines.

When a line is overloaded, the system operator (TSO) asks some generators to reduce their output (down-regulation) and others to increase it (up-regulation), preserving total energy balance. Generators are compensated for deviations from their market schedule; the total payment is the **re-dispatch cost**.

Following Papavasiliou [11] (Definition 5.12), this process is formalised as an optimisation problem in which the TSO selects the cheapest set of adjustments that restore network feasibility. Under the cost-based re-dispatch assumption adopted throughout this thesis (generators bid at their marginal cost), the problem reduces to a DC optimal power flow (DCOPF), as shown in the next section.

2.2.2 Mathematical Model

General Formulation

The re-dispatch problem is first posed in its most general form [13]. Given the zonal market outcome (p_g^*, d_l^*), the TSO seeks adjustments $(\Delta p_g, \Delta d_l)$ that maximise the residual social surplus (the area under demand minus the area under supply) subject to the physical network constraints. Denoting the re-dispatched generation as $\tilde{p}_g = p_g^* + \Delta p_g$ and the re-dispatched demand as $\tilde{d}_l = d_l^* + \Delta d_l$, the general formulation reads:

$$\max_{\Delta p,\, \Delta d,\, r,\, f} \quad \sum_{l \in \mathcal{L}} \int_0^{\tilde{d}_l} MB_l(x)\, dx \; - \; \sum_{g \in \mathcal{G}} \int_0^{\tilde{p}_g} MC_g(x)\, dx \tag{RD}$$

s. t.:

$$r_n = \sum_{g \in \mathcal{G}_n} \tilde{p}_g - \tilde{d}_n \qquad \forall\, n \in \mathcal{N} \tag{20}$$

$$f_k = \sum_{n \in \mathcal{N}} F_{kn}\, r_n \qquad \forall\, k \in \mathcal{K} \tag{21}$$

$$\sum_{n \in \mathcal{N}} r_n = 0 \tag{22}$$

$$-\mathrm{TC}_k \le f_k \le \mathrm{TC}_k \qquad \forall\, k \in \mathcal{K} \tag{23}$$

$$P_g - \tilde{p}_g \ge 0 \qquad \forall\, g \in \mathcal{G} \tag{24}$$

$$D_l - \tilde{d}_l \ge 0 \qquad \forall\, l \in \mathcal{L} \tag{25}$$

Here $\mathcal{N}$ is the set of buses, $\mathcal{G}_n \subseteq \mathcal{G}$ the set of generators at bus n, $\mathcal{L}$ the set of loads, and $\mathcal{K}$ the set of transmission lines. F_{kn} is the entry of the PTDF matrix giving the fraction of a unit injection at bus n that flows through line k (F_{kn}= PTDF$_{kn}$ in Section 2.1.2). P_g and D_l are the installed capacity and maximum demand, respectively, and TC$_k$ is the thermal limit of line k. The variable r_n is the net power injection at bus n into the transmission network. f_k is the physical power flow on line k.

This general formulation is similar to the zonal pricing model (ZPFB), but operates at the nodal level, net positions are now defined at individual buses rather than at the zone level, and line flows are constrained by full thermal limits TC$_k$ rather than by remaining available margins.

Reduction to DCOPF

Under the assumption of inelastic demand ($\Delta d_l = 0$), the demand adjustment drops out and the welfare maximisation becomes a cost minimisation. Setting $\tilde{p}_g = p^*_g + \Delta p_g$ (total output), the general formulation (RD)–(25) reduces to the **DC optimal power flow** (DCOPF), referred to professor Lété [13]:

$$\min_{p,\, r} \quad \sum_{g \in \mathcal{G}} c_g \, \tilde{p}_g \tag{26}$$

s. t.:

$$(\rho_n): \quad r_n \;=\; \sum_{g \in \mathcal{G}_n} \tilde{p}_g - D_n \qquad \forall\, n \in \mathcal{N} \tag{27}$$

$$(\varphi): \quad \sum_{n \in \mathcal{N}} r_n \;=\; 0 \tag{28}$$

$$(\lambda_k^+): \quad \sum_{n \in \mathcal{N}} F_{kn}\, r_n \;\le\; \mathrm{TC}_k \qquad \forall\, k \in \mathcal{K} \tag{29}$$

$$(\lambda_k^-): \quad \sum_{n \in \mathcal{N}} F_{kn}\, r_n \;\ge\; -\mathrm{TC}_k \qquad \forall\, k \in \mathcal{K} \tag{30}$$

$$0 \;\le\; \tilde{p}_g \;\le\; P_g \qquad \forall\, g \in \mathcal{G} \tag{31}$$

where $f_k = \sum_n F_{kn} r_n$ has been substituted directly into the thermal bounds, eliminating f_k as an explicit variable. The dual variable $\rho_n(t)$ of constraint (27) is the locational marginal price (LMP) at bus n: it measures the marginal cost of serving one additional megawatt of demand at that location.

Adaptations to the Implemented Model

Three modifications specialise the DCOPF to the context of this thesis.

(i) Effective demand: Non-dispatchable renewable generators and the frozen battery schedule (see adaptation (ii)) are treated as fixed injections rather than decision variables. Denoting the aggregate renewable output at bus n and period t as $R_n(t)$, and the net battery injection allocated to bus n as bat$_n(t)$ (positive when discharging), the effective demand is defined as:

$$D_n^{\text{eff}}(t) \;=\; D_n(t) \;-\; R_n(t) \;-\; \text{bat}_n(t) \tag{32}$$

Replacing D_n with $D_n^{\text{eff}}(t)$ in constraint (27) accounts for all fixed injections at once, keeping only the dispatchable generation p_g as a decision variable.

(ii) Frozen battery schedule: The battery charging and discharging schedule is determined upstream by the zonal pricing optimisation. At the re-dispatch stage, the net battery injection $p^*_{\text{bat}}(t)$ is treated as a fixed input, distributed across the buses of the relevant zone in proportion to each bus's load share. It enters the model exclusively through $D_n^{\text{eff}}(t)$ and is not a decision variable.

(iii) Handling infeasibility via VOLL: For certain operating conditions (e.g. large renewable surpluses coinciding with congested transmission corridors), the DCOPF may be infeasible: no combination of dispatchable outputs satisfies both the nodal balances and all thermal limits simultaneously. Following professor Lété's recommendation [13], a **Value of Lost Load** (VOLL) is introduced on the demand side. A non-negative load-shedding variable $d_{\text{shed},n}(t) \geq 0$ is added at each bus, representing emergency demand curtailment at cost VOLL per MWh. The implemented formulation becomes:

$$\min_{p,\, r,\, d_{\text{shed}}} \quad \sum_{g \in \mathcal{G}} c_g \, \tilde{p}_g(t) \; + \; \text{VOLL} \cdot \sum_{n \in \mathcal{N}} d_{\text{shed},n}(t) \tag{33}$$

s. t.:

$$(\rho_n): \quad r_n(t) - \sum_{g \in \mathcal{G}_n} \tilde{p}_g(t) - d_{\text{shed},n}(t) \; = \; -D_n^{\text{eff}}(t) \qquad \forall\, n \in \mathcal{N} \tag{34}$$

$$(\varphi): \quad \sum_{n \in \mathcal{N}} r_n(t) \; = \; 0 \tag{35}$$

$$(\lambda_k^+): \quad \sum_{n \in \mathcal{N}} F_{kn} \, r_n(t) \; \leq \; \text{TC}_k^+ \qquad \forall\, k \in \mathcal{K}_c \tag{36}$$

$$(\lambda_k^-): \quad \sum_{n \in \mathcal{N}} F_{kn} \, r_n(t) \; \geq \; -\text{TC}_k^- \qquad \forall\, k \in \mathcal{K}_c \tag{37}$$

$$0 \; \leq \; \tilde{p}_g(t) \; \leq \; P_g \qquad \forall\, g \in \mathcal{G} \tag{38}$$

$$d_{\text{shed},n}(t) \; \geq \; 0 \qquad \forall\, n \in \mathcal{N} \tag{39}$$

where $\mathcal{K}_c \subseteq \mathcal{K}$ is the subset of lines whose thermal capacity is strictly finite (lines marked as unconstrained in the dataset are excluded from the flow constraints). The VOLL parameter is set to its lower-bound European reference value, as estimated by the CEPA study commissioned by ACER [17]. Shedding occurs only when no feasible physical dispatch exists, in all other hours the optimal $d^*_{\text{shed},n}(t) = 0$. No slack is added to line flow constraints: the thermal bounds (36)–(37) are enforced as hard constraints [13].

2.2.3 Two Redispatch Methods

Two variants of the model above are compared in this thesis, differing only in whether the aggregate net position of the zone of interest $\mathcal{Z}$ is constrained to its zonal market value. Let $\mathcal{N}_{\mathcal{Z}} \subseteq \mathcal{N}$ denote the set of buses belonging to zone $\mathcal{Z}$, and let $r^*_{\mathcal{Z}}(t)$ denote the net position of that zone in the zonal pricing solution (positive = net export).

Method A: unconstrained DCOPF

Method A solves (33)–(39) with no additional constraints. All generators in the system are decision variables, and cross-zonal redispatch is allowed: the optimiser can freely shift generation across zone boundaries to minimise total adjustment cost. This provides an idealised lower bound on re-dispatch cost, corresponding to a hypothetical fully coordinated redispatch in which all system operators act as a single entity.

$$\text{Solve (33)–(39) with no additional constraints.} \tag{RD-A}$$

Method B: DCOPF with zone constraint

Method B adds a single constraint that fixes the net position of zone $\mathcal{Z}$ to its zonal market value:

$$\sum_{n \in \mathcal{N}_{\mathcal{Z}}} r_n(t) \; = \; r^*_{\mathcal{Z}}(t) \qquad \forall\, t \tag{40}$$

All generators in the system remain decision variables, but only internal re-dispatch is permitted: cross-zonal exchanges are fixed at their day-ahead market values, and zone $\mathcal{Z}$ must resolve its internal congestion without modifying its net import/export balance. This reflects the standard practice in European re-dispatch, where inter-zonal allocations from the day-ahead market are generally preserved.

$$\text{Solve (33)–(39) with (40) additionally imposed.} \tag{RD-B}$$

Re-dispatch cost

The annual re-dispatch cost under Method A and Method B is defined respectively as

$$C^A = \sum_{t=1}^{8760} C^{\mathrm{rd},A}(t), \qquad C^B = \sum_{t=1}^{8760} C^{\mathrm{rd},B}(t),$$

where $C_{\mathrm{rd}}(t)$ denotes the Belgian generation cost adjustment at hour t, as defined explicitly in Section 3.3.2. Because Method B imposes an additional constraint on the feasible set relative to Method A, its optimal value satisfies $C^B \geq C^A$. Both series are computed for each battery scenario and reported throughout Section 2.

2.2.4 Implementation

Just as we do for the zonal model(ZPFB), the redispatch model is implemented in Julia using the JuMP modelling language and the HiGHS LP solver. The PTDF matrix $F \in \mathbb{R}^{|\mathcal{K}|\times|\mathcal{N}|}$ is computed once before the simulation loop: the bus susceptance matrix B_{bus} is assembled from the network data, the row and column corresponding to the slack bus are removed, the reduced matrix B_{red} is inverted, and the PTDF entries are obtained by equation (9). The effective demand matrix $D^{\mathrm{eff}} \in \mathbb{R}^{|\mathcal{N}|\times T}$ is similarly pre-computed for all periods.

Both LP structures (RD-A and RD-B) are built once: variables (p_g, r_n, $d_{\mathrm{shed},n}$), objective, and constraint patterns are fixed. At each period, only the right-hand sides of the nodal balance constraints are updated to $-D_n^{\mathrm{eff}}(t)$ via `set_normalized_rhs`, and for Method B the zone constraint RHS is additionally updated to $r^*_{\mathcal{Z}}(t)$. Rebuilding the full model at every period is thereby avoided, substantially reducing computation time.

2.3 Batteries

The previous two sections have established the modelling framework: zonal pricing determines which generators run and at what cost, and re-dispatch corrects the resulting schedule to respect the physical limits of the transmission network. Batteries are now introduced into this framework. The central question of this thesis is whether battery storage **increases or decreases intra-zonal congestion**, and if so by how much (measured through the re-dispatch cost).

This section explains how batteries are treated in each modelling step, which scenarios are simulated, and why the re-dispatch cost is the appropriate metric for answering that question.

2.3.1 Role of Batteries in the Modelling Framework

A battery storage unit is a flexible asset: it can consume electricity (charge) or inject electricity (discharge) at any hour, subject to limits on power and energy. Its economic value comes from temporal arbitrage: it absorbs electricity when it is cheap and plentiful, and releases it when it is scarce and expensive.

In this thesis, batteries are integrated into the two-step framework as follows.

Step 1: Zonal pricing: Batteries participate in the zonal market as price-taking agents. Each battery is modelled as a flexible unit that the market dispatch optimises jointly with conventional generators. Because the zonal model ignores all internal network constraints (copper-plate assumption), a battery can freely absorb power and inject it back at any time, without any risk of creating congestion. The outcome of this step is a **battery dispatch profile** $p_b^*(t)$ for each hour of the year, positive when discharging and negative when charging.

Step 2: Re-dispatch: In the re-dispatch step, the battery profile $p_b^*(t)$ computed in Step 1 is treated as fixed. The TSO cannot modify it. The battery behaves exactly like a source with a known hourly profile: its net injection at its physical bus is known in advance and is incorporated directly into the effective nodal demand, as detailed in Section 2.3.4.

This distinction between the two steps is the central modelling hypothesis of this thesis and is discussed in detail in Section 2.3.3.

2.3.2 Scenarios

Five scenarios are simulated, corresponding to different levels of battery deployment. The capacity figures are drawn from Elia's Adequacy and Flexibility Study [3], which provides projections for both small-scale (residential and commercial) and large-scale (grid-connected) battery storage.

Case 0: No storage: This is the baseline: no battery units are present. All results from the zonal and re-dispatch models serve as the reference against which all battery scenarios are compared.

Case 1: Currently installed capacity (2025–2026): Approximately 0.7 GW of small-scale batteries were already installed by 2025, with an additional volume of large-scale batteries contracted under the CRM mechanism. The total assumed capacity is **0.8 GW** of power with a storage duration of 2 hours (energy capacity: 1.6 GWh). This case represents the grid as it exists today.

Case 2: Near-to-medium term (2028–2030): By 2030, AdeqFlex projects approximately 1.0 GW of small-scale batteries under the Current Commitments scenario, combined with large-scale batteries contracted under CRM auctions and commissioned by 2028. The total assumed capacity is **2.5 GW** of power (energy: 5.0 GWh). This case captures the step change introduced by the first large-scale battery tranche.

Case 3: Long term — Prosumer Power scenario (2035): Under the Prosumer Power scenario of AdeqFlex, small-scale residential batteries grow substantially alongside increased prosumer penetration.

Combined with large-scale grid-connected units, the total assumed capacity reaches **3.9 GW** of power (energy: 7.8 GWh). This case represents the upper end of the plausible deployment range within a high-prosumer future.

Case 4: Long term — System stress scenario (2035): This case considers a scenario in which batteries are called upon to fill a large adequacy gap, with ambitious deployment of both small- and large-scale storage. The total assumed capacity is **6.0 GW** of power (energy: 12.0 GWh). This case serves as a stress test: it probes whether very large battery deployments, optimised at the zonal level without regard for network constraints, remain beneficial from a re-dispatch perspective.

The five cases are summarised in Table 1.

Table 1: Battery scenarios simulated in this thesis. Storage duration is assumed to be 2 hours in all cases.

Case	Label	Power (MW)	Energy (MWh)	Reference horizon
0	No storage	0	0	—
1	Currently installed	800	1 600	2025–2026
2	Near-to-medium term	2 500	5 000	2028–2030
3	Long term (PP)	3 900	7 800	2035
4	Long term (stress)	6 000	12 000	2035

Geographic placement

All batteries are located in the Belgian zone. Their total power capacity is distributed across Belgian buses in proportion to each bus's share of the national load. This reflects the assumption that storage (both large-scale grid-connected units and aggregated residential systems) tends to be deployed where electricity consumption is highest.

2.3.3 A Subtlety on Welfare and the Choice of Metric

The apparent paradox

A natural question is: why not allow the TSO to re-dispatch batteries in addition to conventional generators? If batteries could be re-dispatched optimally, one can show that the total social welfare achieved by the two-step procedure would equal the welfare of a **nodal pricing** model, in which the market is cleared subject to all network constraints from the outset [11]. Under nodal pricing, adding more storage capacity can only increase welfare, since it expands the feasible set. It would follow that batteries are always grid positive, which would be a trivial and uninteresting conclusion.

Why batteries are not re-dispatched

In practice, TSOs do not re-dispatch battery storage for a fundamental economic reason: batteries have no well-defined marginal cost. A conventional generator has a fuel cost per MWh that determines how much it should be paid when asked to increase or decrease output. A battery, by contrast, has only opportunity costs: discharging now means less energy available later, and the value of that future discharge depends on future prices that are not yet known at the time of re-dispatch. Pricing this opportunity cost is technically complex and practically unworkable within the pay-as-bid auction framework used by European TSOs.

For this reason, the working hypothesis of this thesis is that **batteries are not available for re-dispatch**. Once the zonal market has cleared and produced a battery dispatch profile $p_b^*(t)$, this profile is treated as fixed in the re-dispatch step. The TSO adjusts only conventional generators, exactly as described in Section 2.2. The adjustment applied to each battery is zero by assumption:

$$\Delta p_b(t) \;=\; 0 \qquad \forall\, b \in \mathcal{B},\; t = 1, \ldots, 8760 \tag{41}$$

Consequence: batteries can be grid negative

This hypothesis has an important implication. The battery profile $p_b^*(t)$, determined by the zonal market without any knowledge of network constraints, creates real power flows on real transmission lines. These flows may increase congestion rather than relieve it. A battery that charges during a period of high renewable generation may draw additional power across already-congested corridors, making re-dispatch more costly. Conversely, a battery discharging during a period of high import may relieve a congested border line.

The outcome depends on the physical location of the battery and the specific pattern of its charge-discharge profile. Batteries are not guaranteed to be grid positive, and determining whether they are in practice, and to what degree, is precisely the question this thesis addresses.

The re-dispatch cost as the comparison metric

Given the hypothesis above, the appropriate metric for comparing scenarios is the re-dispatch cost C^{rd}, defined in Section 2.2.3. It measures the extra cost the TSO must incur to correct the zonal dispatch after batteries have already fixed their profile. A lower re-dispatch cost means batteries have decreased congestion; a higher one means they have made things more costly.

Total welfare comparisons across scenarios would conflate two effects: the benefit of temporal arbitrage (which batteries always provide in the zonal model, regardless of network effects) and the network impact (which is what this thesis is measuring). By focusing on re-dispatch cost, we isolate the network effect—the part that is directly relevant for a TSO's investment and regulatory decisions.

2.3.4 Mathematical Formulation

Battery model in the zonal pricing step

A battery $b \in \mathcal{B}$ is connected to zone $z(b)$ and characterised by its maximum power $P_b^{\max}$ (MW) and its energy capacity E_b (MWh). Both charge and discharge efficiencies are set to 0.95:

$$\eta^c \;=\; \eta^d \;=\; 0.95 \tag{42}$$

Three variables are introduced per battery and per hour:

$$c_b(t) \;\geq\; 0 \qquad \text{charging power (MW, consumed from the grid)} \tag{43}$$
$$d_b(t) \;\geq\; 0 \qquad \text{discharging power (MW, injected into the grid)} \tag{44}$$
$$e_b(t) \;\in\; [0,\, E_b] \qquad \text{state of charge (MWh)} \tag{45}$$

The state of charge evolves from one hour to the next according to:

$$e_b(t) \;=\; e_b(t-1) \;+\; \eta^c \cdot c_b(t) \;-\; \frac{d_b(t)}{\eta^d} \qquad t = 1, \ldots, 8760 \tag{46}$$

The battery is initialised at half its energy capacity at the start of the year and must return to that same level at the end:

$$e_b(0) \;=\; e_b(8760) \;=\; 0.5 \cdot E_b \tag{47}$$

Power bounds apply to both charging and discharging:

$$c_b(t) \;\leq\; P_b^{\max}, \qquad d_b(t) \;\leq\; P_b^{\max} \tag{48}$$

The net injection of battery b at hour t is:

$$p_b(t) \;=\; d_b(t) \;-\; c_b(t) \tag{49}$$

This term enters the zonal energy balance of zone $z(b)$ as an additional source when positive (discharging) and as an additional load when negative (charging). The zone balance constraint from the zonal pricing model is updated to account for the battery net injection:

$$r_z(t) = \sum_{g \in \mathcal{G}_z} p_g(t) + \sum_{b \in \mathcal{B}_z} \big(d_b(t) - c_b(t)\big) - D_z^{\text{net}}(t) \qquad \forall\, z \in \mathcal{Z} \tag{50}$$

where $\mathcal{B}_z$ is the set of batteries in zone z. Because batteries have no fuel cost, they enter the objective function with a marginal cost of zero. The optimiser uses them purely to reduce total system cost: they absorb cheap off-peak generation and release it during expensive peak hours.

Battery treatment in the re-dispatch step

After the zonal model has been solved, the optimal battery profiles $c_b^*(t)$ and $d_b^*(t)$ are extracted. The net battery injection at the physical bus $n(b)$ of battery b is taken as a fixed input:

$$\text{bat}_n(t) \;=\; d_b^*(t) \;-\; c_b^*(t) \tag{51}$$

Its fixed injection is incorporated into the effective nodal demand (32), already defined in Section 2.1.2:

$$D_n^{\text{eff}}(t) \;=\; D_n(t) \;-\; \text{R}_n(t) \;-\; \text{bat}_n(t) \tag{52}$$

The re-dispatch nodal balance (34) then applies unchanged. In Case 0, $\text{bat}_n(t) = 0$ for all n and t, and the battery has no effect on the re-dispatch problem. No battery variable appears in the re-dispatch optimisation: the entire effect of the battery passes through the right-hand side, consistent with hypothesis (41).

3 Simulation and Results

3.1 Case Study: Belgian Re-dispatch in the CWE Market

The general framework developed in the previous sections is applied to the **Central Western European (CWE) electricity market** for the calendar year **2018**. The CWE market comprises five bidding zones: Austria (AT), Belgium (BE), Germany-Luxembourg (DE/LX), France (FR), and the Netherlands (NL). These zones are coupled through the Flow-Based Market Coupling (FBMC) mechanism, in which cross-border capacities are determined by Power Transfer Distribution Factors (PTDFs) and Remaining Available Margins (RAMs) computed from a reference network model.

Choice of zone of interest

Belgium is chosen as the zone of interest $\mathcal{Z}$ throughout this thesis. As a structurally **import-dependent** zone, its generation fleet is dominated by nuclear power operating at near-baseload levels, leaving the system reliant on cross-border imports to meet peak demand. The year 2018 is characterised by significant unplanned nuclear outages, which increased both import dependence and price volatility, making it a stress-test year for congestion management and a meaningful setting in which to evaluate the impact of battery storage.

Network and market structure

The physical network used in the nodal re-dispatch model consists of 632 buses and 944 transmission lines spanning the five CWE zones. Of these, 405 lines have thermal limits below the unconstrained threshold and are enforced as binding constraints in the DCOPF; the remainder never bind under realistic conditions and are excluded. The 19 cross-border lines are retained in all cases as primary indicators of inter-zonal congestion.

The zonal FBMC model operates on the same five zones, with net positions coupled through flow-based parameters derived from the same network. Belgium comprises 24 buses, which host both conventional generators and the battery units described in Section 2.3.

Reference year and simulation horizon

The simulation covers all 8,760 hours of 2018. The zonal pricing model is formulated over the full annual horizon, as the state-of-charge dynamics of the battery couple consecutive hours and prevent decomposition into independent subproblems. The re-dispatch model, by contrast, has no inter-temporal coupling once the battery schedule is fixed: each hourly LP is solved independently after the zonal solution has been obtained.

Key metric

The central outputs of the analysis are the annual Belgian re-dispatch costs C^B and C^A, computed for each battery scenario as defined in equation (RD-A), (RD-B). For each scenario $k \in \{1, 2, 3, 4\}$, the values of C_k^B and C_k^A are compared to the no-battery baseline C_0^X to assess whether battery deployment increases or decreases the cost of restoring network feasibility. The net economic balance is obtained by weighing the Belgian zonal generation-cost saving against the change in re-dispatch cost under each method, yielding a single figure that quantifies the overall impact of battery deployment on the Belgian electricity system.

3.2 Dataset CWE 2018

All simulations in this thesis are based on a power-system dataset covering the Central Western Europe (CWE) region for the reference year 2018. The dataset was originally constructed for the study by Lété, Smeers, and Papavasiliou [18] and covers the five CWE bidding zones: Austria (AT), Belgium (BE), Germany and Luxembourg (modelled as a single zone, DE/LX), France (FR), and the Netherlands (NL). It includes the full high-voltage transmission network, all generation units with their technical and economic parameters, and hourly time series for load and renewable generation over the 8 760 hours of the year.

The dataset is structured around four components: buses, generators, lines, and time-series profiles. Each is described in the following subsections.

3.2.1 Buses

A bus represents a high-voltage substation in the transmission network: it is the physical point at which generators, loads, and transmission lines connect. The dataset contains **632 buses** distributed across the five bidding zones as shown in Table 2.

Table 2: Number of buses per bidding zone.

Zone	Countries	Buses
AT	Austria	36
BE	Belgium	24
DE/LX	Germany and Luxembourg	231
FR	France	317
NL	Netherlands	24
Total		**632**

The spatial resolution is highly uneven across zones. France and Germany together account for 548 of the 632 buses (87%), reflecting the detailed representation of their large high-voltage networks. Luxembourg is included in the DE/LX zone and does not have any dedicated buses separate from the German network.

Each bus is assigned to exactly one bidding zone. In the zonal pricing model, the zone assignment determines which generators and loads belong to the same copper-plate node. In the re-dispatch model, it is used to identify Belgian buses when distributing the battery profile (see Section 2.2).

3.2.2 Generators

Conventional generators

The dataset includes **892 conventional generating units** whose output can be freely chosen by the market within their capacity limits. Table 3 and 4 summarises the fleet by zone and by technology.

Table 3: Conventional generating capacity by zone.

Zone	Units	Capacity (MW)	Share
AT	17	5 640	2.8%
BE	79	12 412	6.3%
DE/LX	634	87 074	44.0%
FR	92	74 391	37.6%
NL	70	18 497	9.3%
Total	**892**	**198 014**	**100%**

Table 4: Conventional generating capacity by technology and marginal cost range.

Technology	**Units**	**Capacity (MW)**	**Share**	**MC (€/MWh)**
Nuclear	73	77 667	39.2%	9.1
CCGT	168	34 819	17.6%	41–68
Coal	93	30 702	15.5%	28–54
OCGT	235	21 558	10.9%	81–115
Lignite	59	20 819	10.5%	18–40
Oil	70	5 772	2.9%	128–185
Other	194	6 078	3.1%	16–39
Total	**892**	**198 014**	**100%**	

Nuclear capacity (77.7 GW) is the largest single technology, almost entirely in France (58 units, around 63 GW) and Belgium (8 units, around 6 GW). With a marginal cost of 9.1 €/MWh in the dataset, nuclear units always rank at the bottom of the merit order and run as base load, which creates the large sustained loop flows through the CWE network that characterise the zonal model (see Section 2.1). Germany has 634 of the 892 units, with a broad mix of lignite, coal, gas, and peaking units. Under the 2003 Nuclear Phase-Out Act, all Belgian reactors were scheduled for closure by 2025 (a deadline subsequently extended for several units) making the long-term availability of Belgian nuclear capacity already uncertain in the 2018 reference year, and lending additional relevance to the question of battery storage as a congestion management resource. This will be covered in Section 3.4, Update of the Dataset.

Belgium's 79 generators are the main subject of this thesis. Their mix is dominated by nuclear (8 units, 5 931 MW), CCGT (21 units, 3 726 MW), OCGT (21 units, 1 555 MW), and a set of oil and other units. Only the marginal variable cost c_g and the installed capacity $P_g^{\max}$ are used in the optimisation models; investment and fixed costs are not relevant for the short-run dispatch problem.

Renewable generators

The dataset includes **1 306 renewable generating units** whose hourly output is determined by a fixed profile, and not by the market. Table 5 shows the fleet by fuel type.

Table 5: Renewable generating fleet by renewable technology (2018 reference year).

RE. Technology	**Units**	**Reference capacity (MW)**	**Share**
Wind (on/offshore)	620	51 095	34.2%
Solar PV	614	46 452	31.1%
Hydraulic (reservoir)	42	38 938	26.1%
Pumped storage	27	12 711	8.5%
Run-of-river hydro	2	127	0.1%
Geothermal	1	8	<0.1%
Total	**1 306**	**149 331**	**100%**

The hourly output of each renewable unit is the product of a reference capacity and a normalised capacity factor profile drawn from the corresponding column of the renewable profiles file. The same profile can be shared across multiple units within a zone, with each unit receiving a fixed fraction (`FractionREProfile`) of the profile's value. This structure allows the dataset to distribute wind and solar generation across multiple buses within a zone while relying on a single aggregate time series per technology and zone.

Pumped-storage hydro units are treated as must-run units with a fixed hourly net profile, consistent with the approach used for all other renewables. Their annual net contribution to the CWE energy balance is slightly negative (−8,496 GWh), reflecting net energy consumed by pumping operations. This is distinct from the BESS scenarios in Section 2.3, which add new dispatchable battery units on top of this fixed baseline.

Table 6: Annual renewable production and penetration by zone (2018).

Zone	Wind (GWh)	Solar (GWh)	Hydro (GWh)	RE penetration
AT	6 396	1 424	30 920	≈ 60%
BE	3 315	3 552	328	≈7%
DE/LX	108 576	41 234	12 683	≈31%
FR	27 804	10 222	50 258	≈19%
NL	3 543	3 082	98	≈6%

Table 6 shows the annual renewable energy production and penetration rate by zone in 2018. Austria stands out with a 60% renewable share, driven by its large reservoir hydro fleet. Germany and France have significant shares from a mix of wind, solar, and hydro, while Belgium and the Netherlands have the lowest penetration in 2018, which makes their dispatchable fleets the main source of flexibility. A comparison with the updated 2025 renewable penetration figures is presented in Section 3.4, where the evolution of the renewable fleet across the two reference years is discussed.

3.2.3 Transmission Lines

The transmission network is composed of **944 lines**, of which 940 are AC and 4 are DC. These split into 925 internal lines (connecting buses within the same zone) and **19 cross-border lines** (connecting buses in different zones).

Table 7: The 19 cross-border lines of the CWE network with their thermal capacities.

Corridor	Line	Type	TC (MW)
AT – DE/LX	A_st.Pet – D-188	AC	1 380
	A_Westti – D_leupol	AC	1 750
	E_obermo – A_Burs	AC	1 370
	E_obermo – A_Burs.(2)	AC	1 370
	D_oberbr – A_Westti	AC	1 520
	A_st.Pet – D-231	AC	900
BE – FR	F-6Aveli – B-12Avel	AC	2 550
	B_Achene – F-12choo	AC	1 490
	B_Moncea – F-12choo	DC	290
	B_Aubang – F_Moulai	AC	762
BE – NL	NL-new1 – B_Zandvl	DC	3 290
	NL_Maasb – B_new1	DC	2 700
BE – DE/LX	B_Aubang – Lx-3	DC	716
DE/LX – FR	F_Vigy – D_185	AC	2 340
	D-185 – F-41	AC	1 000
	F_113 – D_Eichst	AC	1 790
DE/LX – NL	NL_Meede – D_Diele	AC	2 740
	NL_Henge – D_Gronau	AC	3 290
	NL_Maasb – D_Siersd	AC	3 290

Table 8: Summary.

Corridor	Lines	TC (MW)
AT – DE/LX	6	8 290
BE – FR	4	5 092
BE – NL	2	5 990
BE – DE/LX	1	716
DE/LX – FR	3	5 130
DE/LX – NL	3	9 320
Total	**19**	

In the re-dispatch model, only lines with a thermal capacity below 5,000 MW are included as active flow constraints in the LP. This threshold selects **405 constrained lines**: all 19 cross-border lines and 386 internal lines (301 in DE/LX, 41 in AT, 23 in BE, 22 in NL, and none in FR). Lines above the threshold are never binding in practice and are excluded to keep the problem tractable. The 19 cross-border lines form 6 physical corridors between the 5 bidding zones. They are the lines most likely to be congested after the zonal market clears. Table 7 lists all 19 lines with their thermal capacities. Table 8 summarises the six corridors.

The DE/LX–Netherlands corridor is the largest, with a combined capacity of 9 320 MW, reflecting the strong physical integration between Germany and the Netherlands. The Belgium–DE/LX corridor is the most constrained, reduced to a single 716 MW DC cable. The four Belgian corridors together determine the physical limits on Belgium's imports-exports and therefore are the most relevant for this thesis.

Note that the Belgium–Netherlands and Belgium–DE/LX corridors consist entirely of DC cables. DC lines are modelled differently from AC lines in the DC power flow approximation: their flows do not follow Kirchhoff's voltage law and are instead directly controllable. In this dataset they are treated as standard lines in the PTDF computation, which is a common simplification when explicit DC converter control is not modelled.

3.2.4 Load Profiles and Demand

Hourly gross load data is provided as a single aggregate time series per zone over the 8 760 hours of 2018. Each zone's total load at hour t is then distributed across individual buses in proportion to each bus's load share (`FractionLoadProfile`), a fixed coefficient taken from the `Loads.csv` file. Belgium has 12 load buses whose fractions sum to exactly 1. Table 9 summarises the key demand statistics by zone for 2018.

Table 9: Annual demand statistics by zone (2018).

Zone	**Annual consumption (TWh)**	**Peak demand (MW)**	**Load factor**
AT	63.6	10 803	67.3%
BE	87.5	13 231	75.5%
DE/LX	512.7	78 327	74.7%
FR	471.3	94 492	56.9%
NL	114.7	18 837	69.5%
CWE Total	**1 249.8**		

France has the lowest load factor (57%) in the dataset, a consequence of its strong seasonal demand profile (very high winter peak). This creates large nuclear export flows through the CWE network during off-peak periods, which are one of the main drivers of the loop flow congestion discussed in Section 2.1. Germany has by far the largest annual consumption (508.6 TWh for the German part of the DE/LX zone plus 4.1 TWh for Luxembourg), reflecting its size and industrial base. Belgium's consumption of 87.5 TWh and peak of 13,231 MW are modest compared to its neighbours, but its central position in the network means its lines carry significant transit flows from France and Germany to the Netherlands, making congestion management particularly relevant.

In the simulations, demand is treated as perfectly inelastic at every hour: consumers purchase whatever quantity is needed regardless of price. This standard assumption is consistent with the cost-minimisation formulation of the zonal pricing model (see Section 2.1).

3.3 Results on CWE 2018

This section presents the simulation results for the five battery scenarios applied to the CWE 2018 dataset. The analysis is organised in three parts: the zonal market outcomes (Section 3.3.1), the re-dispatch costs under both methods (Section 3.3.2), and the combined net economic impact (Section 3.3.3). In all tables and figures, Case 0 denotes the baseline without any battery storage; Cases 1 through 4 correspond to installed Belgian BESS capacities of 800 MW, 2 500 MW, 3 900 MW, and 6 000 MW respectively. The 3 900 MW and 6 000 MW scenarios represent the lower and upper bounds of Elia's 2035 adequacy and flexibility projection [3].

3.3.1 Zonal market outcomes

Price per zone

Figure 1 shows the annual average zonal price for each bidding zone and each battery scenario. The dominant feature is the large and persistent price spread between zones. In Case 0, France averages 14.8 €/MWh while Belgium averages 55.6 €/MWh — a gap of approximately 41 €/MWh, or roughly 74% of the Belgian price. This spread reflects the structural excess of French nuclear generation and the near-permanent saturation of the FR↔BE interconnection corridor. The three remaining zones fall between these extremes: DE/LX at 38.3 €/MWh, NL at 47.2 €/MWh, and AT at 48.7 €/MWh. Prices across the five zones are equalised for fewer than 100 hours per year, confirming that cross-border congestion is almost continuous throughout 2018.

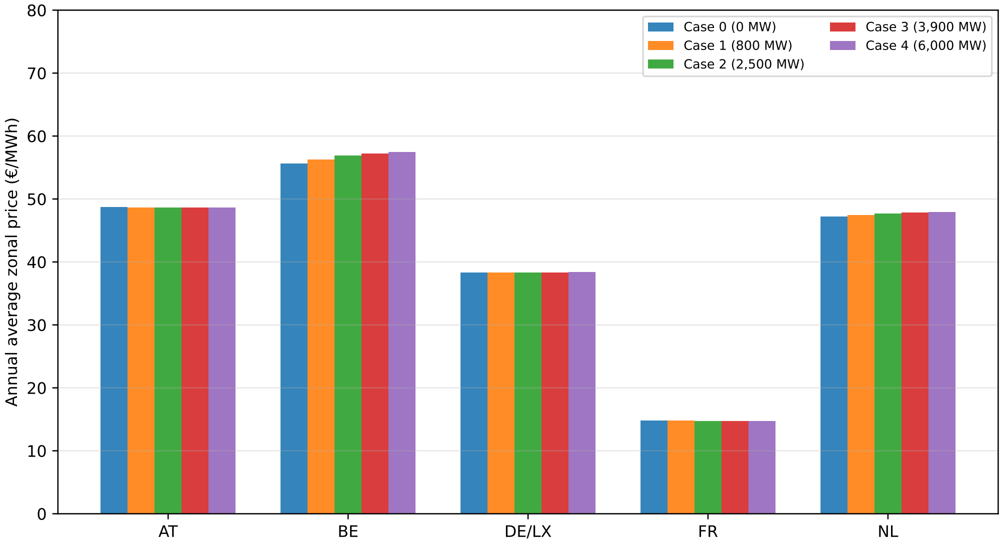

Figure 1: Annual average zonal price by bidding zone and battery scenario (2018).

Battery deployment has a small but consistent upward effect on the Belgian average price, which rises from 55.6 €/MWh in Case 0 to 57.5 €/MWh in Case 4 (+3.4%). At first sight this appears paradoxical: one might expect batteries to suppress prices by injecting power during peak periods. The explanation lies in the role of cross-border flows and net imports. The simulation shows that Belgium's annual net import position increases from 17 290 GWh in Case 0 to 18 234 GWh in Case 4, an increase of approximately 944 GWh (+5.5%).

Two mechanisms explain this price increase. First, batteries operate at a round-trip efficiency of 95 %, meaning they consume slightly more energy during charging than they release during discharge. For Case 4, this loss amounts to roughly 221 GWh per year, which must be covered by additional generation or imports, marginally tightening supply. Second, during low-price hours, batteries charge by absorbing energy that Belgium would otherwise have exported to neighbouring zones. In the CWE flow-based model, cross-border flows are physically coupled: reducing Belgium's net export position tightens both the FR↔BE and NL↔BE corridors, which are already congested for the vast majority of 2018 hours. The Netherlands, receiving less energy via the Belgian node, must dispatch its own more expensive domestic generators — which is why a small but consistent price increase is also observed in NL across all battery cases.

France's average price of 14.8 €/MWh lies well above the marginal cost of nuclear generation (≈9 €/MWh) for a structural reason: in the zonal model, exports count as demand that France must serve. France's total net output (domestic consumption plus cross-border exports) exceeds what cheap nuclear alone can supply, so France must dispatch additional, more expensive generators whose marginal cost sets the zonal price. If France had to export nothing, its domestic demand could largely be met by nuclear alone and its price would approach the nuclear floor. On the other hand, the congestion on the FR↔BE corridor primarily affects Belgium, not France: it prevents Belgium from accessing sufficient cheap French energy and forces it to rely on its own more expensive generators, sustaining the persistent price differential between the two zones.

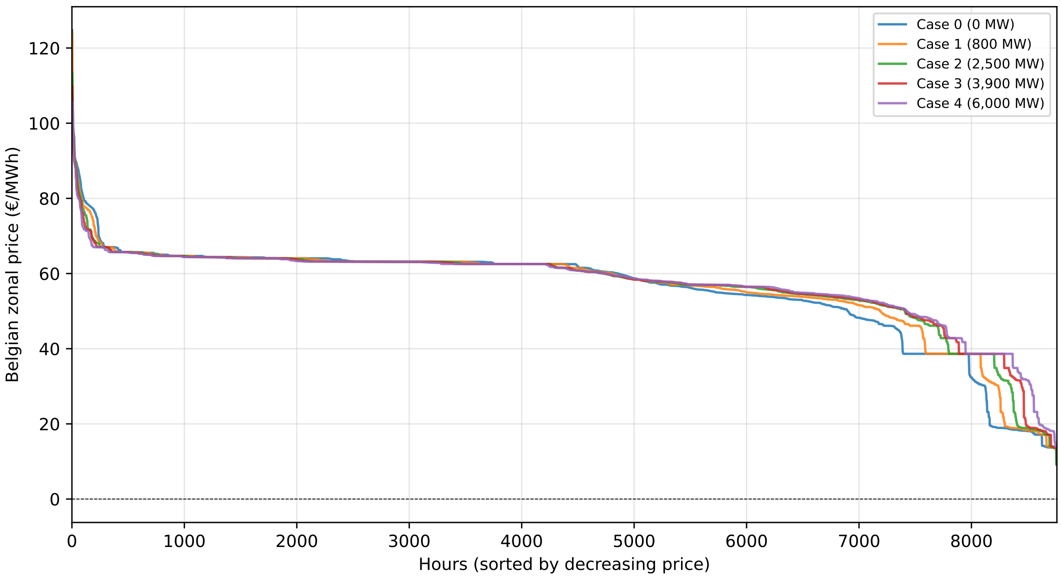

Figure 2: Belgian price duration curve for all battery scenarios (2018).

Figure 2 shows the Belgian price duration curve (Hours sorted in decreasing price order) for all five scenarios. Three observations stand out:

First, the curves for Cases 1 through 4 overlap almost perfectly with Case 0 for the 7,000 most expensive hours: batteries leave the upper portion of the price distribution essentially unchanged, confirming that they do not dampen peak prices. Second, the five curves diverge sharply in the right-hand tail (hours 7,000–8,760), which corresponds to the cheapest hours of the year. In Case 0, prices approach zero during these hours as excess supply finds no outlet; in Case 4, batteries absorb this surplus during charging, raising the price floor to approximately 15–20 €/MWh. Third, this selective lifting of the price floor is precisely what the standard deviation captures: it measures how dispersed hourly prices are around their annual average. Since batteries compress only the bottom of the distribution while leaving the top unchanged, the spread narrows — the standard deviation falls from 14.0 €/MWh in Case 0 to 10.3 €/MWh in Case 4, a reduction of 27 %. No negative prices occur in any scenario, consistent with a 2018 generation mix in which Belgian nuclear reliably covers baseload demand.

Battery behaviour

Figure 3 shows the average net hourly injection of Belgian batteries by hour of day. A clear two-valley charging pattern is visible: batteries charge between approximately 22:00 and 05:00 (overnight low-demand hours) and again around 11:00—13:00 during the midday demand trough. They discharge during the morning demand ramp (06:00–10:00) and the evening peak (15:00–20:00). This pattern is driven by the typical intraday price structure of Central European electricity markets and is consistent across all capacity scenarios; larger batteries scale the same profile rather than shifting it in time.

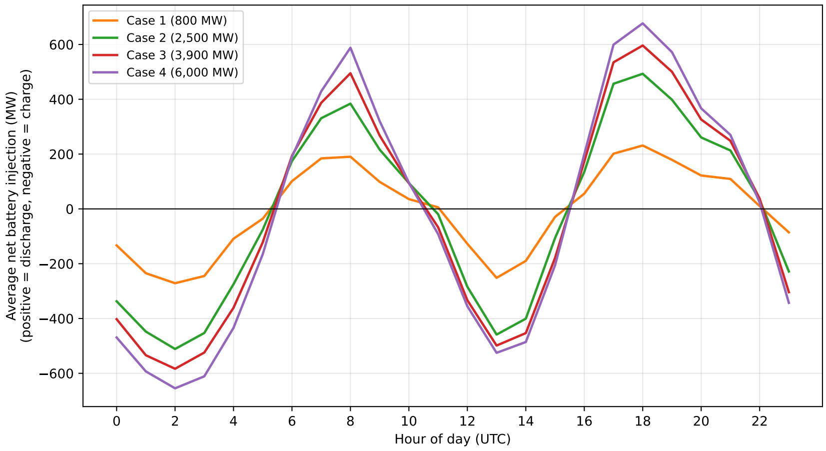

Figure 3: Average net battery injection by hour of day for Cases 1–4 (2018).

System cost savings

Table 10 summarises the key zonal market performance indicators. Belgian generation costs fall monotonically from 801 M€/year in Case 0 to 746 M€/year in Case 4 (-6.8%), driven by batteries displacing expensive domestic gas-fired generation during peak hours. The savings exhibit clear diminishing returns: the first 800 MW reduces Belgian generation costs by 17.9 M€/year (−2.2%), while the step from 3 900 MW to 6 000 MW yields only an additional 8.8 M€/year (−1.1%). The arbitrage spread (the difference between the average Belgian price during discharge hours and during charge hours) confirms this saturation: it falls from 15.1 €/MWh in Case 1 to 10.4 €/MWh in Case 4 (−31%), as increasing capacity competes for the same limited price differentials.

These savings are computed over all 8 760 hours of the simulation year. For the net-impact comparison in Section 3.3.3, however, zonal savings are restricted to the hours for which the re-dispatch model also yields a feasible solution (approximately 6 850 hours per year), so that both cost components are evaluated over an identical set of operating conditions. The resulting *comparable* zonal savings are reported in Table 12.

Table 10: Zonal market performance by scenario (2018). Belgian generation cost savings are relative to Case 0 (801 M€/year).

Case	Battery (MW)	BE gen. cost (M€/yr)	Saving vs C0 (M€/yr, %)	Throughput (GWh/yr)	Arb. spread (€/MWh)
0	0	801.0	—	—	—
1	800	783.0	−17.9 (−2.2%)	634	15.1
2	2 500	763.0	−38.0 (−4.7%)	1 375	11.8
3	3 900	755.1	−45.9 (−5.7%)	1 717	10.9
4	6 000	746.2	−54.7 (−6.8%)	2 039	10.4

3.3.2 Re-dispatch costs

The re-dispatch costs reported in this section measure the net additional cost attributable to Belgian generators at the re-dispatch stage, relative to their output at the zonal market clearing:

$$C_{\mathrm{BE}}^{X} = \sum_{g \in \mathcal{G}_{\mathrm{BE}}} c_g \cdot \left(q_g^X(t) - p_g^*(t)\right), \qquad X \in \{A, B\},$$

where c_g is the variable cost (€/MWh) of generator g, $p_g^*(t)$ its dispatched output at the zonal market-clearing stage, $q_g^X(t)$ its output after re-dispatch under method X, and $\mathcal{G}_{\mathrm{BE}}$ the set of Belgian generators. The difference $q_g^X(t) - p_g^*(t)$ is the net change in output imposed on generator g at hour t by the re-dispatch optimisation: positive values correspond to upward re-dispatch (the generator produces more than at the zonal stage), and negative values to downward re-dispatch.

This quantity is summed over all feasible hours of the year; a positive annual total indicates that Belgian generators incur a net extra cost relative to the market schedule, i.e. expensive up-regulation outweighs the credit from cheap down-regulation. Hours for which the re-dispatch model yields no feasible solution are excluded: approximately 1 900 hours per year, concentrated in January, February, and December, were flagged as infeasible. These correspond to extreme winter congestion events — precisely the operating conditions under which battery charging most aggravates already-loaded corridors. Restricting the analysis to the remaining feasible hours therefore constitutes a best-case scenario for batteries: the cost increments reported below are lower bounds on the true annual re-dispatch impact. The fact that batteries remain grid-negative even under this favourable selection strengthens rather than weakens the conclusion. This limitation is discussed further in Section 4.

Method A vs. Method B annual costs

Figure 4 and Table 11 present the annual Belgian re-dispatch costs under both methods for each scenario. The baseline figures (Case 0) reveal an important asymmetry: $C_{\mathrm{BE}}^{B} = 222\,\mathrm{M€/year}$ whereas $C_{\mathrm{BE}}^{A} = 356\,\mathrm{M€/year}$, making Method A 60% more expensive for Belgium despite being the globally optimal solution. This apparent paradox is resolved by understanding what each method optimises.

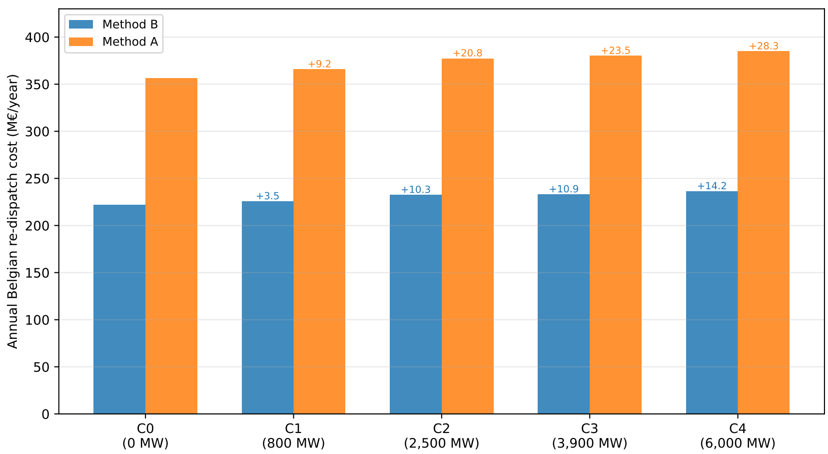

Figure 4: Annual Belgian re-dispatch cost by scenario and method (2018). Annotations show the absolute change relative to Case 0.

Method A minimises total CWE-wide re-dispatch costs using generators from all six countries simultaneously. The globally optimal solution calls Belgian generators upward more intensively than their cross-border counterparts, because Belgian units are geographically positioned to relieve transit flows across the Belgian grid at the lowest system-wide cost. The savings from down-regulating generators elsewhere in Europe accrue to those countries, not to Belgium. Method B, by contrast, fixes Belgium's net import–export position and restricts the optimiser to intra-Belgian adjustments; many CWE-wide violations remain partially unresolved, so Belgian generators are called upon less aggressively and the net Belgian cost is lower. In practice, the true Belgian re-dispatch cost lies somewhere between these two bounds, depending on the degree of cross-border TSO coordination actually achieved.

Table 11: Annual Belgian re-dispatch cost by scenario and method (2018). Percentage changes are relative to Case 0.

Case	Battery (MW)	C^B (M€/yr)	Change vs C0 (M€/yr, %)	C^A (M€/yr)	Change vs C0 (M€/yr, %)
0	0	222.0	—	356.4	—
1	800	225.5	+3.5 (+1.6%)	365.6	+9.2 (+2.6%)
2	2 500	232.3	+10.3 (+4.6%)	377.2	+20.8 (+5.8%)
3	3 900	232.9	+10.9 (+4.9%)	379.9	+23.5 (+6.6%)
4	6 000	236.2	+14.2 (+6.4%)	384.7	+28.3 (+7.9%)

Battery deployment increases the Belgian re-dispatch cost monotonically under both methods. Under Method B, the cost rises from 222 M€ in Case 0 to 236 M€ in Case 4, an increase of 14.2 M€/year (+6.4%). Under Method A, the increase is larger in absolute terms but similar in relative terms: from 356 M€ to 385 M€ (+28.3 M€, +7.9%). The increment grows rapidly up to 2 500 MW and then more slowly for the larger scenarios: from Case 2 to Case 4, Method B costs rise by only 3.9 M€ despite adding 3 500 MW of capacity (−73% per MW compared to Case 0–2).

This pattern suggests that marginal re-dispatch impact of additional battery capacity diminishes as the system adjusts to the new injection geography.

Seasonal distribution

Figure 5 shows the monthly Belgian re-dispatch costs for both methods and all five scenarios. The seasonal pattern is consistent: costs appear lowest in January (5–6 M€ under Method B) (partly because January and February contain a disproportionate share of the ∼1 900 infeasible hours, so the most extreme winter stress events are excluded from the monthly totals) and peak sharply in November (51 M€ under Method B, approximately 85 M€ under Method A before falling slightly in December. This winter peak reflects high heating demand and the surge in large cross-border import flows traversing the Belgian high-voltage grid, which load internal corridors and require significant generation adjustments.

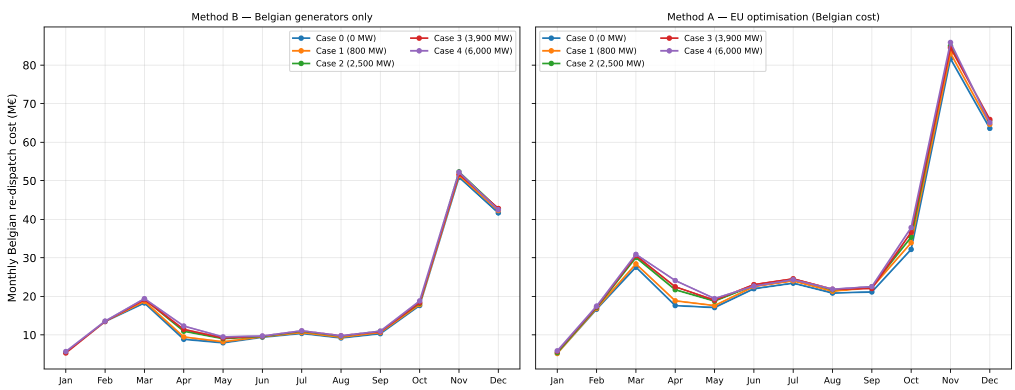

Figure 5: Monthly Belgian re-dispatch costs for Method B (left) and Method A (right).

Crucially, the five scenarios trace nearly identical seasonal profiles in both panels: battery deployment shifts the cost level slightly upward but does not alter the timing or structure of congestion across the year. Batteries therefore affect the magnitude of re-dispatch interventions, not their underlying seasonal drivers.

Why batteries increase re-dispatch costs

The mechanism behind the cost increase stems from how batteries interact with the Belgian generation fleet without coordination with the TSO. As specified in Section 2.3, battery schedules are fixed by the zonal market optimisation (which has no knowledge of intra-zonal network constraints) and are not available to the TSO at the re-dispatch stage.

When batteries charge, they inject additional demand at Belgian load buses, tightening the constraints on nearby transmission lines. The TSO responds by curtailing local generation, primarily the two dispatchable Belgian nuclear units (Doel 4 and Tihange 3). Under Method B, the annual downward re-dispatch of these units increases from 878 GWh in Case 0 to 958 GWh in Case 1 (+9.1%), before moderating slightly for larger capacities. When batteries discharge, they inject power at Belgian nodes during peak hours, reinforcing the outbound power flows on corridors that are already heavily loaded. To restore feasibility, the TSO must ramp up expensive gas-fired units located downstream of the congested lines. Since the marginal cost of upward gas re-dispatch exceeds the compensation for nuclear curtailment, the net Belgian re-dispatch cost rises.

3.3.3 Combined results

Figure 6 and Table 12 decompose the net economic impact of each battery scenario into the Belgian generation cost saving achieved at the zonal stage — restricted to re-dispatch-feasible hours for comparability (see Section 3.3.1) — and the additional re-dispatch cost imposed at the network stage.

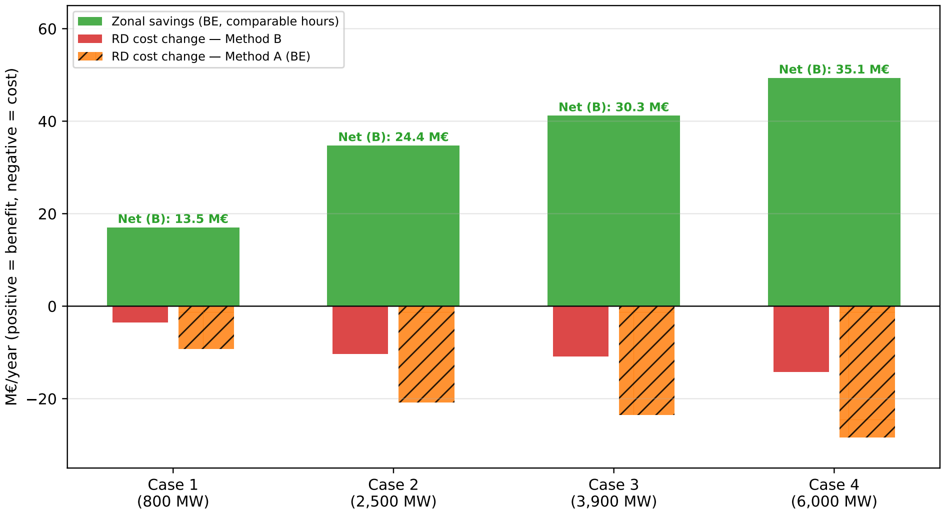

Figure 6: Net economic impact of battery deployment **relative to Case 0** (2018). Green bars show Belgian zonal savings over re-dispatch-feasible hours only; red and orange bars show the incremental re-dispatch cost under Method B and Method A respectively. The set of feasible hours differs between Method A and Method B for a given scenario, so zonal savings and Method A cost increments are not evaluated over an identical set of hours. Net benefit annotations therefore refer strictly to Method B, for which savings and cost increment are evaluated over the same comparable hours.

The primary result visible in Figure 6 is straightforward: battery deployment raises Belgian re-dispatch costs in every scenario and under both accounting methods. This confirms that price-arbitrage BESS is *grid-negative* in the 2018 dataset — the central answer to the research question. The red and orange bars in Figure 6 rise above zero regardless of capacity level or accounting method; there is no scenario in which batteries relieve congestion costs.

Table 12: Decomposition of the net economic impact of battery deployment (M€/year relative to Case 0, 2018). Zonal savings are restricted to feasible hours only for Method B (approximately 6 850 h/yr), ensuring direct comparability with the Method B re-dispatch cost increment ΔC_B. The feasible-hour set for Method A differs from that of Method B; Method A values are provided for reference only and do not correspond to the same hours as the reported zonal savings.

Case	Battery (MW)	Zonal saving* (M€/yr)	RD change (B) (M€/yr)	Net (B) (M€/yr)	RD change (A) (M€/yr)	Net (A) (M€/yr)
1	800	+17.0	+3.5	+13.5	+9.2	+7.8
2	2 500	+34.7	+10.3	+24.4	+20.8	+14.0
3	3 900	+41.2	+10.9	+30.3	+23.5	+18.0
4	6 000	+49.3	+14.2	+35.1	+28.3	+20.9

*Comparable hours only; full 8 760 h savings in Table 10.

A secondary, and reassuring, finding is that the net economic balance remains positive across all scenarios. Under Method B, the re-dispatch penalty represents a modest fraction of the comparable zonal benefit: 21% in Case 1, rising to 29% in Case 4. The net benefit grows from 13.5 M€/year at 800 MW to 35.1 M€/year at 6 000 MW (+160% across the full capacity range), with diminishing marginal returns consistent with the saturation of arbitrage opportunities identified in Table 10.

Under Method A, the picture is less favourable for Belgium. Because the CWE-wide optimiser calls heavily on Belgian generators to resolve CWE-wide congestion, the Belgian re-dispatch cost absorbs approximately 54% of the comparable zonal benefit in Case 1 and 57% in Case 4. The net benefit under Method A remains positive but smaller: from 7.8 M€/year (Case 1) to 20.9 M€/year (Case 4).

This asymmetry between the two methods has an important practical interpretation. Method B cannot resolve all CWE-wide violations using Belgian generators alone, so the uncorrected residual congestion is effectively borne by the grid; the Belgian fleet does less total work, and the Belgian cost share is lower. Method A resolves congestion fully, but the least-cost solution disproportionately leverages Belgian generators — and the associated cost is borne by Belgian consumers rather than distributed across the CWE region. This points to a structural feature of the current market design: under full TSO coordination, Belgium would bear a larger share of the CWE re-dispatch bill than its size would suggest, simply because of its central geographic position in the transmission grid.

Reconciling the price paradox

The combination of a rising average Belgian price (+3.4 % from Case 0 to Case 4) and a positive net economic impact may seem contradictory. Two effects compete: when batteries discharge at peak hours they replace expensive gas peakers and push prices down; when they charge during cheap hours they tighten already-congested cross-border corridors and push prices up. In 2018, near-permanent corridor congestion means the second effect slightly dominates on the annual average. However, the average price is not the right welfare metric. Gas peakers displaced at peak carry marginal costs of roughly 150 €/MWh, while the stored energy was purchased at 30–40 €/MWh; the saving per peak-hour is large. The corridor effect, by contrast, raises the average price by only 1–2 €/MWh spread thinly across all hours. Belgian generation costs therefore fall by 6.8 % even as the average price rises by 3.4 %: batteries arbitrage intertemporal price differences, and the value recovered at peak far exceeds the cost of the average price nudge upward.

Summary of key findings (2018)

Building on the above, the central findings of this section are as follows. A first structural finding deserves emphasis before discussing magnitudes: price-arbitrage BESS is *grid-negative* in the 2018 dataset — that is, batteries systematically <u>increase</u> total re-dispatch costs relative to the no-storage baseline in every scenario and under both accounting methods. Second, batteries operated without network awareness consistently increase re-dispatch costs, but the increment is modest — at most 6.4 % of the Case 0 baseline under Method B and 7.9 % under Method A. Third, the net economic impact remains strongly positive across all scenarios: under the operationally realistic Method B, additional re-dispatch costs absorb at most 29 % of the zonal benefit, leaving a net gain of 13.5–35.1 M€/year. Finally, the analysis highlights a structural asymmetry in the current European market design: under full TSO coordination (Method A), Belgium bears a disproportionate share of CWE-wide re-dispatch costs — a policy question that deserves attention as BESS capacity continues to scale up.

Taken together, these results provide a first affirmative answer to the thesis's central question: price-arbitrage BESS generates a positive net economic benefit for Belgium even when re-dispatch costs are internalised, and this holds across all capacity scenarios and both accounting methods. The following section examines whether these findings hold in a structurally different 2025 market, where higher renewable penetration fundamentally alters both the arbitrage opportunity and the re-dispatch landscape.

3.4 Update of the Dataset to 2025

The baseline dataset described in Section 3.2 reflects the CWE power system as it stood in 2018. However the European electricity sector has gone through structural change in the lasts years:

- Germany completed its nuclear phase-out in April 2023
- Belgium revised its policy by extending two reactors while retiring the rest of its fleet
- France closed Fessenheim and commissioned the long-delayed Flamanville 3 EPR
- France and the Netherlands finalised their coal exits
- The ALEGrO HVDC cable between Belgium and Germany entered service in 2020.

On the supply side, renewable capacity across the CWE region has grown dramatically, with solar PV installations more than tripling in most zones and offshore wind expanding significantly. On the demand side, total consumption has modestly declined compared to 2018, reflecting the effects of energy efficiency measures and the 2022 energy crisis.

Applying the 2018 dataset to a 2025 research question would overstate German nuclear capacity and understate renewable penetration, two factors central to CWE cross-border flows and congestion. The dataset has therefore been updated to 2025 using publicly available data from the ENTSO-E Transparency Platform [19, 20] and other national sources detailed below.

The update covers five components: the conventional generation fleet (`Generators.csv`), the transmission network (`Lines.csv`), the hourly load profiles (`LoadProfiles.csv` and `Loads.csv`), and the renewable generation profiles (`RenewableProfiles.csv` and `GeneratorsRE.csv`). The bus list (`Buses.csv`), reserve requirements (`Reserves.csv`), and all techno-economic parameters (costs, start-up types) are left unchanged.

3.4.1 Conventional Generators

The conventional generation fleet was revised to reflect the power plant closures and additions that occurred between 2018 and 2025. All modifications were applied directly to the `Generators.csv` file, on a unit-by-unit basis. Table 13 summarises the changes by country and technology. Negative values indicate capacity retirements; positive values indicate additions.

Table 13: Changes to the conventional generation fleet (2018 → 2025).

Zone	**Units**	**Cap. (MW)**	**Plants**
Nuclear retirements			
DE/LX	−6	−8 114	Isar 2, Grohnde, Brokdorf, Gundremmingen C, Emsland, Neckarwestheim 2
BE	−6	−3 854	Doel 1, Doel 2, Doel 3, Tihange 1 (N+S), Tihange 2
FR	−2	−1 760	Fessenheim 1, Fessenheim 2
Nuclear additions			
FR	+1	+1 630	Flamanville 3 (EPR)
Coal retirements			
FR	−4	−2 650	Cordemais 4+5, Emile Huchet 6, Le Havre 4, Provence 5
NL	−5	−2 952	Hemweg 7, Hemweg 8, Hemweg 9, Amercentrale 8, Amercentrale 9

These changes reflect a combination of national energy policy decisions, regulatory commitments, and ageing plant closures, each of which is detailed in the following paragraphs.

German nuclear phase-out

Germany's *Atomausstieg* (nuclear phase-out) proceeded in two steps during this period. On 31 December 2021, the second-to-last group of reactors was shut down: Grohnde (1 360 MW, operated by PreussenElektra), Brokdorf (1 410 MW, PreussenElektra), and Gundremmingen C (1 288 MW, RWE) [21]. The three remaining reactors, Isar 2 (1 410 MW, E.ON), Emsland (1 336 MW, PreussenElektra), and Neckarwestheim 2 (1 310 MW, EnBW), were originally scheduled for closure in December 2022 but received a three-month extension due to the 2022 European energy crisis. They were permanently disconnected on 15 April 2023, ending nuclear electricity generation in Germany [22]. In total, six nuclear units corresponding to 8 114 MW of capacity were removed from the DE/LX zone (see Table 13).

Belgian nuclear policy

Belgium's nuclear policy was substantially revised in 2023. Under the original phase-out law of 2003, all seven Belgian nuclear units were to close by 2025. In April 2024, however, the Belgian federal parliament passed a law extending the operating licences of Doel 4 (1 039 MW) and Tihange 3 (1 038 MW) by ten years until 2035 [23]. The remaining five units (Doel 1 (433 MW), 2 (433 MW), 3 (1 006 MW), Tihange 1 (two half-units totalling approximately 920 MW), and 2 (1 000 MW)) closed as scheduled. Belgian nuclear capacity therefore falls from six units (5 931 MW in 2018) to two units (2 077 MW in 2025), a reduction of 3 854 MW [24] (see Table 13).

French nuclear: Fessenheim closure and Flamanville 3 addition

In France, two changes occurred in opposite directions. The Fessenheim nuclear plant (the oldest in the French fleet, commissioned in 1977) was shut down in two steps: unit 1 (880 MW) on 22 February 2020 and unit 2 (880 MW) on 30 June 2020, following a long-standing government commitment [25]. Both units have been removed. Partially offsetting this reduction, the Flamanville 3 EPR (European Pressurised Reactor) was connected to the French grid on 21 December 2024 after more than fifteen years of construction delays and cost overruns [26, 27]. With a rated capacity of 1 630 MW, it is France's first new nuclear unit. Flamanville 3 has been added to the dataset at bus F-34, assigned the same marginal cost and SLOW start-up type as the other French nuclear units, and inserted immediately before Flamanville 1 and 2 in the generator list. The net effect on French nuclear capacity is $-1{,}760 + 1{,}630 = -130$ MW (see Table 13).

French coal phase-out

France committed to ending coal-fired electricity production by 2022. While some plants received temporary extensions for energy security reasons during the 2022 crisis, all four remaining French coal units had permanently ceased commercial operation by the end of 2024 [28, 29]: Cordemais 4 and 5 (EDF, Loire-Atlantique), Emile Huchet 6 (GazelEnergie, Moselle), Le Havre 4, and Provence 5. All four have been removed from the `Generators.csv` file, which represents a reduction of 2 650 MW (see Table 13).

Dutch coal closures

The Netherlands decreed a law in 2019 banning the use of coal for electricity generation [30]. The immediately affected plants were the older, less efficient units in Amsterdam. Hemweg 7 (585 MW), operated by Vattenfall, was shut down in late 2017 and, while physically offline, remained listed in the 2018 baseline dataset; it has accordingly been removed in this update. Hemweg 8 (650 MW) was permanently closed on 23 December 2019 following a Dutch court ruling [31]. Hemweg 9 (432 MW), the last unit of the Hemweg complex, ceased operation before 2025. Similarly, Amercentrale 8 (645 MW) and 9 (640 MW) in Geertruidenberg, owned by RWE, ceased coal generation by the end of 2024; unit 9 has since converted to run entirely on biomass [32].All five Dutch coal units have been removed. Note that the Maasvlakte 3 and Rotterdam coal plants, which are newer and more efficient, remained operational in 2025 and are still in the dataset. All the retirements represents a reduction of 2 952 MW (see Table 13)

Updated fleet summary

After all modifications, the 2025 conventional fleet comprises **868 generating units**, vs. 892 in 2018. Table 14 compares the conventional generation capacity by zone between the 2018 and 2025 datasets, for each technology. CCGT, OCGT, Lignite, and Oil capacities are unchanged between the two years and are aggregated under "Other".

Table 14: Conventional generating capacity by zone: 2018 vs. 2025 (GW).

	Nuclear		**Coal**		**Other**		**Total**	
Zone	**2018**	**2025**	**2018**	**2025**	**2018**	**2025**	**2018**	**2025**
AT	0	0	1.08	1.08	4.57	4.57	5.65	5.65
BE	5.93	2.08	0	0	6.47	6.47	12.40	8.55
DE/LX	8.11	0	22.69	22.69	54.90	54.90	85.70	77.59
FR	63.13	63.00	2.65	0	8.33	8.33	74.11	71.33
NL	0.49	0.49	4.78	1.82	13.0	13.0	18.27	15.31
CWE	**77.66**	**65.57**	**31.20**	**25.59**	**87.27**	**87.27**	**196.1**	**178.4**

The disappearance of German nuclear generation is the most consequential structural change in the conventional fleet (-8 GW), followed by the Belgian, French and Nederlands reduction of conventional generators by ≈3 GW each. With zero nuclear capacity in 2025, Germany becomes a net importer during high-demand periods, altering the direction and magnitude of cross-border flows throughout the CWE region.

3.4.2 Transmission Lines

From 2018 to 2025, only one significant interconnector was added to the network: the ALEGrO (Aachen–Liège Electricity Grid Overlay) HVDC cable connecting Belgium and Germany. ALEGrO was commissioned in October 2020 and is operated jointly by Elia (Belgium) and Amprion (Germany). It links bus B-11 (near Lixhe, Belgium) to bus D-136 (near Oberzier, Germany) with a rated capacity of 1 000 MW in each direction [33, 34].

Before ALEGrO, the Belgium–Germany corridor consisted of a single DC cable (B_Aubang–Lx-3, 716 MW), making it by far the most constrained corridor in the CWE network. ALEGrO roughly doubles the BE–DE/LX interconnection capacity, from 716 MW to 1 716 MW. The new line has been added to `Lines.csv` as an AC line (the DC power flow formulation treats it identically to other lines) with the identifier `B-11.To.D-136_ALEGRO`.

The 2025 network thus comprises **945 lines** vs. 944 in 2018: 941 AC and 4 DC, with the pre-existing 4 DC lines (covering the BE–FR, BE–NL, and BE–DE/LX corridors) unchanged.

3.4.3 Load Profiles and Demand

Hourly actual total load data for 2025 were downloaded from the ENTSO-E Transparency Platform for each of the five zones [19]. Germany and Luxembourg are loads are reported as a combined bidding zone (DE-LU); the Luxembourg share was separated using a fixed fraction of 1.3%, derived from historical load data, yielding a Luxembourg annual consumption of approximately 6.1 TWh, consistent with Eurostat figures.

The raw ENTSO-E files are in 15-minute resolution. They were resampled to hourly averages, filtered to the calendar year 2025 (8 760 hourly intervals), and linearly interpolated over the small number of missing values (fewer than ten per zone, which is negligeable). The resulting time series replace the 2018 profiles in `LoadProfiles.csv`. The static `Loads.csv` file, which distributes each zone's load across individual buses in fixed proportions, was updated by recomputing the reference value for each bus entry as the product of its fixed fraction and the new 2025 zonal peak. Table 15 compares key demand statistics between the 2018 and 2025 datasets.

Table 15: Annual demand statistics by zone: 2018 vs. 2025.

Zone	**Annual consumption (TWh)**		**Peak demand (MW)**	
	2018	**2025**	**2018**	**2025**
AT	63.6	59.2	10 803	10 402
BE	87.5	80.2	13 231	13 031
DE/LX	512.7	470.7	78 327	76 400
FR	471.3	434.7	94 492	86 646
NL	114.7	116.9	18 837	19 556
CWE	**1 249.8**	**1 161.7**		

Consumption declined in four of the five zones relative to 2018, with reductions ranging from −3.7% in Austria to −7.8% in France. The French peak demand fell by 8.3%, (from 94.5 GW to 86.6 GW), largely reflecting the combined effect of mild winters, structural improvements in building insulation, and reduced industrial activity. The Netherlands is the only zone where both energy and peak demand rose slightly (+1.9% and +3.8% respectively), driven primarily by the growth of electric vehicle adoption and data centre load. Overall, CWE total consumption fell by approximately 7% (from 1 250 TWh to 1 162 TWh). The load factor and seasonal profile of each zone remain qualitatively similar to 2018. The inelastic demand assumption used in the optimisation models is retained.

3.4.4 Renewable Generators

As the demand, the wind and solar generation time series were updated to 2025 actual values using the ENTSO-E Transparency Platform dataset "Actual Generation per Production Type" [20]. For each zone, a long-format CSV file was downloaded containing 15-minute resolution data for all production types. The relevant types extracted for this work are Solar, Wind Onshore, and Wind Offshore. The raw data were pivoted to wide format, resampled to hourly averages, filtered to calendar year 2025, and linearly interpolated over isolated missing values before replacing the corresponding columns in `RenewableProfiles.csv`. It is exactly the same method as for the demand profiles.

A special case arises for the Netherlands. ENTSO-E solar data for the TenneT NL (Nederlands TSO) control area are largely unavailable in the Transparency Platform for 2025 due to reporting gaps. Solar generation for the Netherlands was therefore estimated using the Renewables.ninja platform [35, 36], which provides satellite- and reanalysis-based hourly capacity factors. A 2019 MERRA-2 hourly profile (35° tilt, south-facing, 10% system loss) was scaled to the 2025 installed Dutch solar capacity of approximately 26 GW [37]. The 2019 meteorological year is used as a representative proxy for the seasonal solar pattern; inter-annual variability in the capacity factor profile is modest compared to the large increase in installed capacity. The resulting profile gives an annual Dutch solar generation of approximately 29.8 TWh, consistent with published national estimates [37].

For all zones, wind and solar values are clipped to zero where the raw data contain small negative values. Hydro generation profiles (reservoir, run-of-river, and pumped-storage net profiles) and geothermal profiles are left unchanged from the 2018 dataset: reservoir and run-of-river hydro are driven by hydrological conditions rather than installed-capacity growth, and geothermal is negligible in the CWE context.

The `GeneratorsRE.csv` file was updated consistently. For each solar or wind generator, the reference value (`ReferenceValueRE`) was recomputed as 105% of the product of the generator's fixed profile fraction and the new 2025 profile peak. This uniform 5% margin (applied consistently across all solar and wind units, in contrast to the heterogeneous reference values of the original dataset) ensures that the reference value is never a binding constraint during the DC optimal power flow, while remaining close to the measured peak. Hydro and geothermal reference values are left unchanged. Table 16 compares the annual renewable energy generation and profile peaks between the 2018 and 2025 datasets. "Peak" is the highest observed hourly output in the profile; "Annual" is the corresponding aggregate yearly energy.

Table 16: Renewable generation profiles: 2018 vs. 2025.

Zone	Technology	Peak (MW)		Annual (TWh)	
		2018	**2025**	**2018**	**2025**
AT	Solar	911	4 672	1.4	5.7
	Wind	2 912	3 645	6.4	8.5
BE	Solar	2 620	7 726	3.6	10.2
	Wind	1 159	4 903	3.3	12.2
DE	Solar	28 955	52 466	41.2	74.2
	Wind	44 628	51 609	108.6	133.4
FR	Solar	6 234	19 434	10.2	30.3
	Wind	12 086	19 560	27.8	48.6
NL	Solar*	2 262	20 618	3.1	29.8
	Wind	900	6 883	3.5	22.7
CWE Solar total				**59.5**	**150.2**
CWE Wind total				**149.6**	**225.5**

* NL solar estimated via Renewables.ninja (2019 MERRA-2, scaled to 26 GW installed).

Renewable generation grew substantially across all CWE zones between 2018 and 2025. CWE-wide solar output more than doubled (+152%) and wind output rose by 51%, with the largest relative gains in the Netherlands, Belgium, and Germany. This higher share of variable generation increases the volatility of power flows and, combined with the loss of German nuclear baseload, is expected to alter both the frequency and location of transmission congestion compared to 2018, reinforcing the relevance of battery storage as a congestion management tool in the present study.

3.4.5 Summary

Table 17 provides a consolidated overview of all changes made to the CWE dataset in the transition from 2018 to 2025.

Table 17: Summary of dataset changes: 2018 → 2025.

File	Change	Source
`Generators.csv`	−6 DE nuclear (−8 114 MW)	[21, 22]
	−6 BE nuclear (−3 854 MW)	[23, 24]
	−2 FR nuclear (−1 760 MW)	[25]
	+1 FR nuclear (+1 630 MW)	[26, 27]
	−4 FR coal	[28, 29]
	−5 NL coal	[30, 31, 32]
`Lines.csv`	+1 BE–DE HVDC line (1 000 MW)	[33, 34]
`LoadProfiles.csv`	8 760 h actual load, 2025	[19]
`Loads.csv`	Reference values recalibrated to 2025 peaks	Derived from above
`RenewableProfiles.csv`	12 wind/solar columns replaced with 2025 data	[20, 35, 36]
`GeneratorsRE.csv`	`ReferenceValueRE` updated for 1 234 units	Derived from above
`Buses.csv`, `Reserves.csv`	Unchanged	—

The updated dataset thus reflects the CWE power system as it stands in 2025: a generation mix with significantly less nuclear and coal capacity, a much larger share of variable renewables, and a reinforced Belgium–Germany interconnection. All other structural elements (bus topology, reserve requirements, and techno-economic parameters) are retained from the validated 2018 baseline.

3.5 Results on CWE 2025

This section presents the simulation results for the five battery scenarios applied to the updated CWE 2025 dataset. The structure mirrors Section 3.3: zonal market outcomes (Section 3.5.1), re-dispatch costs under both methods (Section 3.5.2), and the combined net economic impact (Section 3.5.3). The same case numbering and capacity levels apply: Case 0 is the no-battery baseline; Cases 1 through 4 correspond to 800 MW, 2 500 MW, 3 900 MW, and 6 000 MW of Belgian BESS respectively.

3.5.1 Zonal market outcomes

Price per zone

Figure 7 shows the annual average zonal prices for the 2025 dataset. The overall price level is lower than in 2018, and the zone ordering has changed significantly. France now averages only 10.6 €/MWh in Case 0, reflecting the combined effect of the Flamanville 3 EPR commissioning, the completion of the French coal exit, and the substantial expansion of wind capacity. Belgium averages 50.5 €/MWh, DE/LX 33.8 €/MWh, NL 41.8 €/MWh, and AT 38.0 €/MWh. The FR↔BE spread therefore remains large (approximately 39.9 €/MWh), driven by the same structural surplus of cheap French generation and corridor saturation as in 2018.

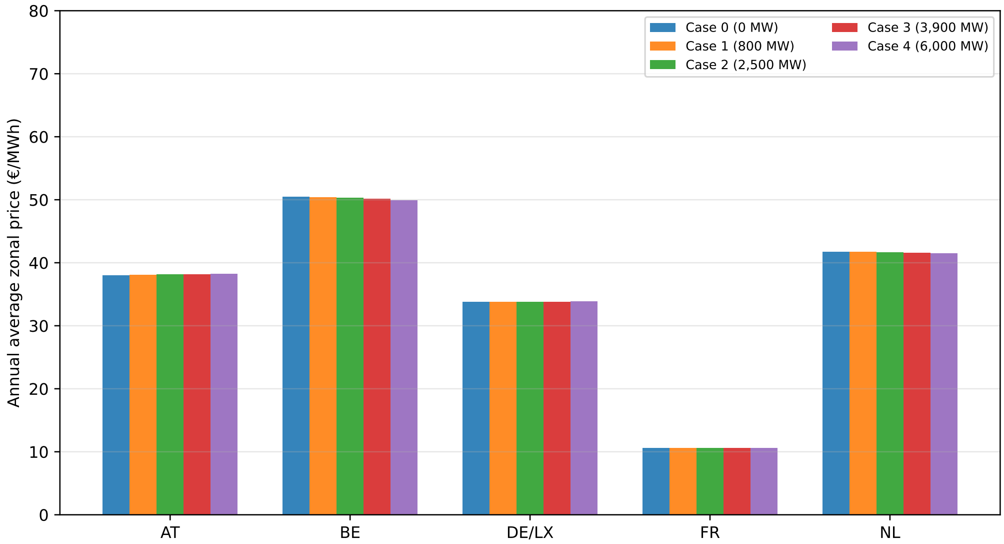

Figure 7: Annual average zonal price by bidding zone and battery scenario (2025).

A notable difference from 2018 is the frequency of price convergence across zones: the five zones share the same price for approximately 520 hours per year in Case 0, compared to fewer than 100 hours in 2018. The ALEGrO HVDC cable and the removal of German nuclear baseload have partially relaxed the most persistent congestion patterns, allowing more frequent price equalisation during periods of low demand and high renewable output.

Battery deployment has a small but consistent downward effect on the Belgian average price, which falls from 50.5 €/MWh in Case 0 to 49.9 €/MWh in Case 4 (−1.2%). This is the opposite direction from 2018, where batteries raised the Belgian price. The inversion reflects a structural shift in the generation mix: in 2025, peak Belgian prices are primarily set by gas-fired units during renewable troughs, and battery discharge during those peak periods suppresses the marginal price directly. The import-congestion channel that dominated in 2018 is still present (net imports increase from 25 942 GWh in Case 0 to 27 193 GWh in Case 4, a rise of 1 251 GWh, or +4.8%), but it is outweighed by the peak-shaving effect.

France's average price of 10.6 €/MWh in 2025 is notably closer to the nuclear marginal cost (≈9 €/MWh) than the 14.8 €/MWh observed in 2018. The mechanism is the reverse of what was described in Section 3.3: in 2018, France's total net output (domestic demand plus cross-border exports) exceeded what cheap nuclear alone could supply, forcing the dispatch of more expensive units that set the zonal price well above the nuclear floor. In 2025, the commissioning of Flamanville 3, the completion of the French coal exit, and the expansion of wind capacity collectively increase the share of cheap generation in the French merit order. At the same time, higher renewable output across the CWE region reduces neighbouring countries' dependence on French exports, so France's net export volume is lower. With a larger cheap generation base and fewer exports to serve, the marginal unit dispatched in France sits closer to the bottom of the merit order — and the French zonal price converges toward the nuclear floor.

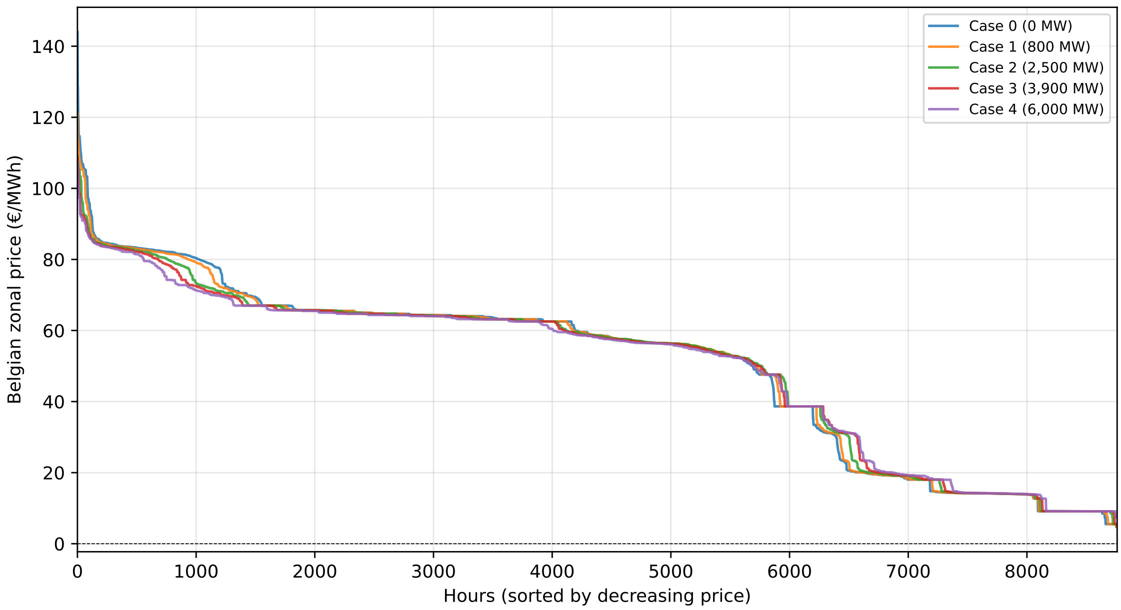

Figure 8: Belgian price duration curve for all scenarios (2025). Hours sorted in decreasing price order.

Batteries also compress the Belgian price distribution, though less dramatically than in 2018: the standard deviation of hourly prices falls from 24.9 €/MWh in Case 0 to 22.9 €/MWh in Case 4, a reduction of only 8 % (versus 27 % in 2018). Figure 8 shows why: in the top-left of the duration curve (the ∼1 500 most expensive hours, above 70 €/MWh), larger battery cases visibly sit below Case 0 — batteries discharge at peak and shave the highest prices. In the right-hand tail, the floor is only marginally raised compared to 2018, because the midday solar surplus is less persistent than the overnight surplus of 2018. The dominant effect in 2025 is therefore peak shaving rather than floor lifting, and the high baseline volatility driven by variable renewables limits how much the battery fleet can smooth the overall distribution.

A direct comparison with observed 2025 price-duration curves would reveal an important limitation of the simulated PDC: the model cannot reproduce the negative prices that increasingly appear in real European markets during periods of excess renewable generation, because the welfare-maximisation dispatch assumes inelastic demand with no demand response or curtailment at negative prices. Furthermore, the perfect-foresight battery dispatch assumed in the simulation yields more favourable cycling than a real operator with imperfect price forecasts, which may slightly exaggerate the price-smoothing visible in the PDC. These points are discussed further in the limitations section.

Battery behaviour

Figure 9 shows the average net hourly battery injection by hour of day for the 2025 dataset. The two-valley charging pattern observed in 2018 is preserved, but with a more pronounced midday charging trough: batteries charge heavily between 10h00 and 14h00, corresponding to the solar generation peak that has grown significantly with the tripling of CWE solar PV capacity since 2018. The overnight charging window (22h00–05h00) remains prominent. The discharge peaks occur during the morning ramp (06h00–10h00) and the evening demand peak (16h00–20h00), consistent with the typical Central European demand profile. Larger battery capacities scale the same intraday profile without shifting its timing, confirming that the arbitrage structure is driven by structural price patterns rather than by strategic behaviour.

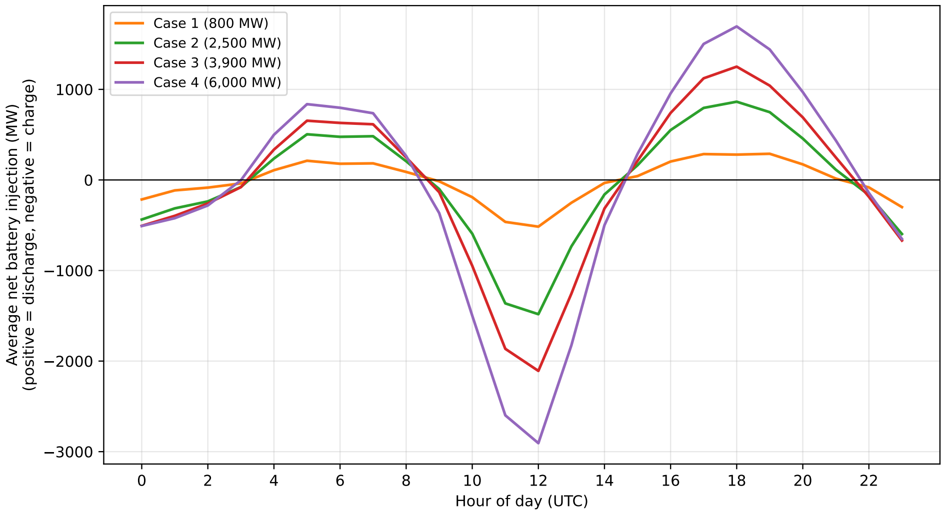

Figure 9: Average net battery injection by hour of day for Cases 1–4 (2025).

System cost savings

Table 18 summarises the zonal market performance indicators. Belgian generation costs fall from 1 028 M€/year in Case 0 to 955 M€/year in Case 4 (−7.2%), driven by batteries displacing expensive gas-fired peakers during high-demand hours and storing cheap midday solar energy. The absolute savings are larger than in 2018 for high-capacity scenarios (73.5 M€ vs. 54.7 M€ at 6 000 MW), reflecting the higher arbitrage spreads available in the more volatile 2025 price environment.

Table 18: Zonal market performance by scenario (2025). Belgian generation cost savings are relative to Case 0 (1 028 M€/year).

Case	Battery (MW)	BE gen. cost (M€/yr)	Saving vs C0 (M€/yr, %)	Throughput (GWh/yr)	Arb. spread (€/MWh)
0	0	1 028	—	—	—
1	800	1 017	−11.0 (−1.1%)	833	32.3
2	2 500	995	−33.3 (−3.2%)	2 244	26.4
3	3 900	978	−50.1 (−4.9%)	3 162	23.8
4	6 000	955	−73.5 (−7.2%)	4 344	21.5

However, the savings for small battery capacities are notably lower than in 2018: the first 800 MW yields only 11.0 M€/year (−1.1%), compared to 17.9 M€/year (−2.2%) in 2018. This apparent paradox is explained by the nature of the 2025 price distribution. While the arbitrage spread is substantially higher (32.3 €/MWh in Case 1 versus 15.1 €/MWh in 2018), the steep price spikes are infrequent and short-lived; a small battery fleet captures fewer cycling opportunities per unit of capacity because the optimal dispatch is concentrated in rare extreme hours. Larger fleets benefit from the full depth of the price distribution, explaining the less pronounced diminishing returns pattern at high capacities.

Note on savings comparability

The savings in Table 18 are computed over all 8 760 hours of the year and correctly reflect the full arbitrage value delivered by each battery scenario in the zonal market. However, approximately 2 950–3 011 hours per year are flagged as infeasible by the re-dispatch optimisation and excluded from its cost accounting (Section 3.5.2). To ensure that zonal savings and re-dispatch costs are compared over an identical set of operating conditions, Section 3.5.3 restricts the zonal savings to the hours that are feasible under both Case 0 and Case k for the corresponding re-dispatch method, yielding approximately 5 750–5 820 comparable hours per year (depending on case and method). For Cases 1–3, the filtered savings deviate by less than 0.5 M€/yr from the full-year figures in Table 18. Case 4 is an exception: the 6 000 MW fleet charges at high rates during the winter high-load hours that are precisely those flagged as infeasible for the re-dispatch model; since battery charging in those hours increases net Belgian generation cost in the zonal model, excluding them raises the apparent Belgian saving from 73.5 M€ to 77.6 M€. This effect is discussed further in Section 3.5.3.

3.5.2 Re-dispatch costs

The re-dispatch cost measure is identical to that used in Section 3.3.2:

$$C_{\mathrm{BE}}^{X} = \sum_{g \in \mathcal{G}_{\mathrm{BE}}} c_g \cdot \left(q_g^X(t) - p_g^*(t)\right), \qquad X \in \{A, B\},$$

summed over all feasible hours. In 2025, approximately 2 950 hours per year were flagged as infeasible and excluded — a marked increase from the 1 900 infeasible hours observed in 2018. This rise reflects the more extreme flow conditions that occur in 2025: with German nuclear removed from the dispatch, large wind and solar surpluses in Germany and France more frequently create transit overloads through the Belgian high-voltage grid that cannot be resolved within the re-dispatch model's constraints. The infeasible count increases slightly with battery capacity (from 2 950 in Case 0 to 3 011 in Case 4), confirming that batteries marginally exacerbate internal congestion.

These excluded hours (the most severe congestion events of the year) are also those in which battery charging would impose the largest additional burden on the re-dispatch system. The cost increments reported below therefore represent a lower bound on the true annual re-dispatch impact: even in this best-case selection of hours, batteries remain grid-negative under both methods and across all four capacity scenarios.

Method A vs. Method B annual costs

Figure 10 and Table 19 present the annual Belgian re-dispatch costs for the 2025 dataset, and reveal a structural inversion relative to 2018.

Under Method B, the baseline cost is $C_{\mathrm{BE}}^{B} = 97.2$ M€/year — less than half the 2018 value (222 M€/year). The reduction reflects the smaller Belgian dispatchable fleet in 2025: with four nuclear units retired, fewer upward re-dispatch calls are needed to resolve internal congestion, and the remaining flexible capacity is cheaper to mobilise.

Under Method A, the 2025 baseline is negative: $C^A_{\mathrm{BE}} = -48.2\,\mathrm{M€/year}$. A negative value means that Belgian generators are net downward-regulated at the re-dispatch stage — they produce less than their market schedule, earning Belgian consumers a cost credit. This inversion is explained by the 2025 flow regime. With German nuclear absent and large volumes of French nuclear and CWE-wide renewable generation flowing eastward and northward, the Belgian high-voltage grid frequently acts as a transit corridor under conditions of oversupply. The CWE-optimal re-dispatch resolves the resulting internal congestion by curtailing Belgian generation (primarily the two retained nuclear units, Doel 4 and Tihange 3, whose output reinforces the overloaded corridors). Since down-regulation of low-cost nuclear units is cheaper than alternative relief measures elsewhere in Europe, the globally optimal solution systematically calls Belgian generators downward, yielding a net cost reduction for Belgium under Method A.

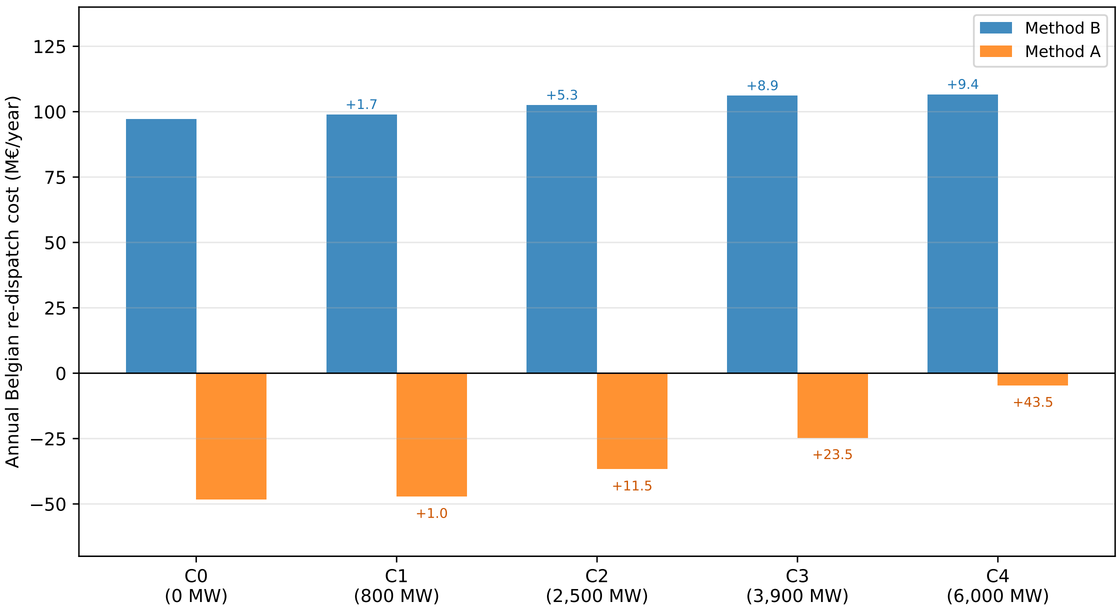

Figure 10: Annual Belgian re-dispatch cost by scenario and method (2025). Annotations show the absolute change relative to Case 0. Method A values are negative in all scenarios, indicating a net cost credit for Belgium.

Table 19: Annual Belgian re-dispatch cost by scenario and method (2025). Percentage changes are relative to Case 0. Negative values of C^A indicate a net cost credit for Belgium.

Case	Battery (MW)	C^B (M€/yr)	Change vs C0 (M€/yr, %)	C^A (M€/yr)	Change vs C0 (M€/yr, %)
0	0	97.2	—	−48.2	—
1	800	98.9	+1.7 (+1.7%)	−47.2	+1.0 (+2.1%)
2	2 500	102.5	+5.3 (+5.5%)	−36.7	+11.5 (+23.8%)
3	3 900	106.1	+8.9 (+9.2%)	−24.7	+23.5 (+48.8%)
4	6 000	106.6	+9.4 (+9.7%)	−4.7	+43.5 (+90.3%)

This is the opposite of 2018, when Method A imposed a 60% cost premium on Belgium because its generators were called upward more than any other zone. The sign flip reflects the structural change in cross-border flows: Belgium has shifted from a net congestion-relief provider (upward regulation in 2018) to a net curtailment target (downward regulation in 2025) under full TSO coordination.

Battery deployment affects both methods, but in opposite directions relative to the 2018 findings. Under Method B, the cost rises from 97.2 M€ in Case 0 to 106.6 M€ in Case 4, an increase of 9.4 M€/year (+9.7%). Under Method A, the cost increases toward zero: from −48.2 M€ to −4.7 M€, a change of +43.5 M€— the Method A benefit is almost entirely eroded by the largest battery scenario. The mechanism in both cases is the same: batteries charging inject additional demand at Belgian load buses, which reduces the net generation surplus and therefore the need for downward regulation of Belgian units. As the battery fleet grows, Belgium transitions progressively from a net downward-regulation target toward a more balanced re-dispatch position.

Seasonal distribution

Figure 11 shows the monthly Belgian re-dispatch costs for both methods and all five scenarios. Under Method B, the seasonal pattern is broadly similar to 2018, with costs peaking in November (approximately 16–17 M€ in Case 0, rising to 50–52 M€ in Case 4) and remaining lower in spring and summer (6–10 M€). A secondary peak in March and April, absent in 2018, reflects the high cross-border flows associated with early spring wind generation in northern Europe. The five scenarios again trace nearly parallel seasonal profiles: batteries amplify the cost level but preserve the underlying seasonal structure.

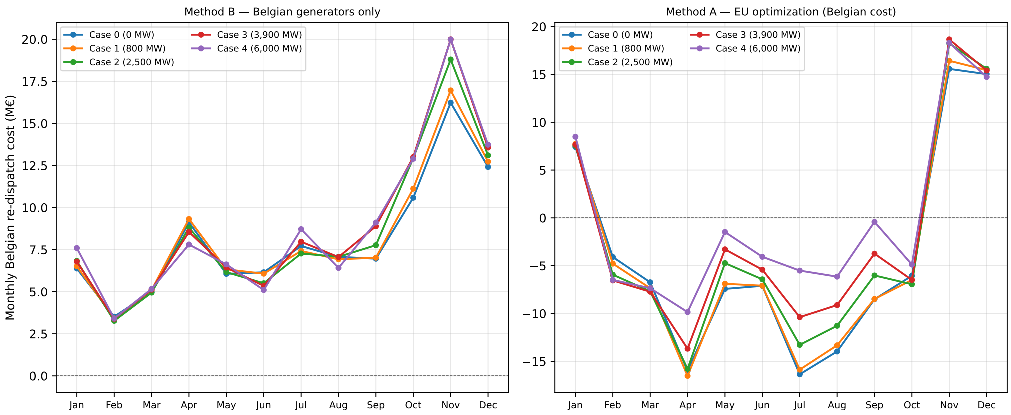

Figure 11: Monthly Belgian re-dispatch costs for Method B (left) and Method A (right), all five battery scenarios (2025). Note that Method A values are predominantly negative (cost credit for Belgium).

Under Method A, all scenarios show negative monthly costs throughout the year in lower-capacity cases, with the benefit concentrating in the November–December peak (approximately −10 M€ per month). As battery capacity grows, this negative profile is progressively eroded: by Case 4, several months in autumn and winter approach or cross zero, indicating a near-complete erosion of Belgium's Method A advantage during the highest-congestion periods.

Why batteries increase re-dispatch costs under Method B

The mechanism is structurally identical to 2018. Battery schedules are determined by the zonal market optimisation, which has no visibility of intra-zonal network constraints, and are therefore fixed at the re-dispatch stage.

When batteries charge, they absorb power at Belgian load buses, tightening the net generation surplus and requiring the TSO to reduce upward curtailment of nearby units or call up additional gas-fired capacity. When batteries discharge, they inject power during peak hours, reinforcing outbound flow on already loaded corridors and forcing the TSO to ramp up expensive gas units downstream of the congested lines. Both effects raise the net Belgian re-dispatch cost under Method B. The retained nuclear units (Doel 4 and Tihange 3) continue to play the central role as the primary down-regulation targets during periods of internal overloading.

3.5.3 Combined results

As in 2018, the primary result of Figure 12 is that battery deployment raises Belgian re-dispatch costs in every scenario and under both accounting methods: price-arbitrage BESS is grid-negative in the 2025 dataset as well. The direction of the congestion effect is unambiguous and consistent across all capacity levels.

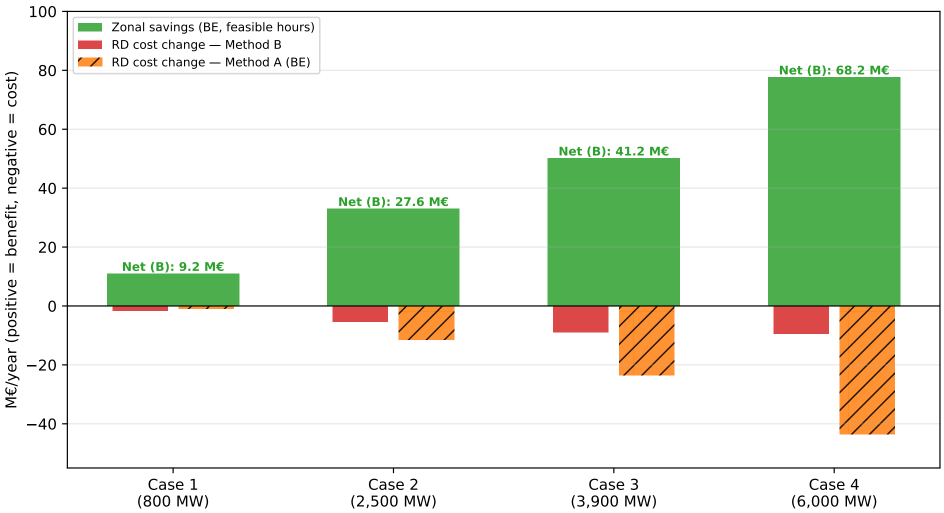

Figure 12: Net economic impact of battery deployment relative to Case 0 (2025). Zonal savings are restricted to feasible hours only under Method B (≈5 750–5 820 h/yr depending on case), ensuring comparability with the Method B re-dispatch cost increment. The feasible hours for Method A differ from those for Method B; net benefit annotations therefore refer strictly to Method B.

Table 20: Decomposition of the net economic impact of battery deployment (M€/year relative to Case 0, 2025). Zonal savings are computed over feasible hours for Method B. For Method A, the RD change represents an erosion of Belgium's re-dispatch cost credit; a positive value therefore indicates a reduced benefit. Note that feasible hours differ between Method A and Method B.

Case	Battery (MW)	Zonal saving (M€/yr)	RD change (B) (M€/yr)	Net (B) (M€/yr)	RD change (A) (M€/yr)	Net (A) (M€/yr)
1	800	+10.9	+1.7	+9.2	+1.0	+9.9
2	2 500	+32.9	+5.3	+27.6	+11.5	+21.5
3	3 900	+50.1	+8.9	+41.2	+23.5	+27.0
4	6 000	+77.6	+9.4	+68.2	+43.5	+33.6

The secondary finding is that the net economic balance remains robustly positive. Under Method B, the net economic impact is positive in all scenarios and grows substantially with capacity. The re-dispatch penalty remains a small and roughly stable fraction of the zonal benefit: 16% in Case 1, falling to 12% in Case 4 — a more favourable ratio than in 2018 (21–29%). The net benefit under Method B reaches 68.2 M€/year at 6 000 MW, compared to 35.1 M€/year in 2018, a 94% increase driven by the higher arbitrage value available in the more volatile 2025 price environment.

Under Method A, the picture is more nuanced. For Case 1 only, Method A is marginally more favourable than Method B (9.9 M€ versus 9.2 M€), because the baseline Method A credit (−48.2 M€) is barely eroded at low battery penetration (+1.0 M€). From Case 2 onwards, however, Method B becomes more favourable and the gap widens rapidly: the Method A erosion absorbs 9% of zonal savings in Case 1 but 56% in Case 4. At 6 000 MW, the net Method A benefit (33.6 M€) is less than half the Method B net benefit (68.2 M€), compared to a 60% ratio in 2018.

This acceleration of Method A erosion with capacity is the most striking new finding of the 2025 analysis. It reflects the non-linear sensitivity of Belgium's downward regulation need to battery charging load: as the battery fleet grows, it progressively fills the generation surplus that would otherwise trigger curtailment of Belgian nuclear units. Once the surplus is absorbed, the TSO must turn to more expensive alternatives, and the cost advantage vanishes. The transition is rapid because the available downward regulation headroom from Doel 4 and Tihange 3 is structurally limited by their combined capacity.

A notable feature of Table 20 is that the filtered zonal saving for Case 4 (+77.6 M€) exceeds the full-year saving reported in Table 18 (+73.5 M€). This apparent paradox arises because the 6 000 MW battery fleet charges at high rates during winter high-load periods — precisely the hours most likely to be flagged as infeasible by the re-dispatch optimisation. During those hours, the large charging demand increases net generation at Belgian load buses in the zonal model, partially offsetting the arbitrage-driven generation cost reduction and producing a negative hourly saving for Belgium. Excluding these infeasible hours therefore removes a set of negative contributions, raising the net filtered figure above the full-year total. This effect is absent in Cases 1–3, where the charging load remains small enough that its hourly cost contribution stays negative throughout the year.

Summary of key findings (2025)

The central findings of this section are the following. First, battery storage continues to generate substantial economic value through temporal price arbitrage in the 2025 generation mix: Belgian generation cost savings reach 73.5 M€/year at 6 000 MW, exceeding the 2018 results at the same capacity, driven by higher intraday price volatility associated with renewable intermittency. Second, under the operationally realistic Method B, the re-dispatch penalty is proportionally smaller than in 2018 (at most 18% of zonal savings), and the net Method B benefit reaches 68.2 M€/year at 6 000 MW. Third, the 2025 re-dispatch landscape is structurally inverted relative to 2018 under Method A: Belgian generators are net downward-regulated in the baseline (−48.2 M€/year), a benefit that batteries progressively erode. At 6 000 MW, 56% of the zonal benefit is absorbed by the erosion of this re-dispatch credit under Method A. Finally, the 2025 results highlight an important asymmetry in the policy implications of battery scaling: while increasing BESS capacity consistently improves the Method B net balance, it disproportionately degrades the Method A position, suggesting that the economic case for large-scale BESS deployment depends critically on the assumed degree of cross-border TSO coordination.

A structural finding cuts across all 2025 scenarios and both accounting methods: price-arbitrage BESS is *grid-negative*, meaning that batteries consistently increase total re-dispatch costs relative to the no-storage baseline. Under Method B (Belgian re-dispatch only), the increment reaches 9.4 € M/yr (+9.7 %) at 6 000 MW (Case 4); under Method A (EU-wide re-dispatch), the erosion of zonal savings is larger in absolute terms, reaching 43.5 € M/yr at Case 4. This grid-negativeness is the direct counterpart of the positive zonal savings: arbitrage flattens the Belgian price profile, which reduces the incentive for cross-border flows and forces system operators to substitute more costly domestic re-dispatch. The net economic balance for Belgium remains positive because the zonal savings outweigh the re-dispatch penalty, but the grid-negative externality grows with installed capacity and points to the need for network-aware battery dispatch or appropriate regulatory incentives.

Taken together, these results confirm that price-arbitrage BESS generates a robustly positive net economic benefit for Belgium in the 2025 market context — and this benefit is substantially larger than in 2018, driven by deeper intra-day price spreads created by the solar duck curve and a structurally lower re-dispatch cost burden. Section 3.6 brings these two pictures together and examines how the economic case for Belgian BESS evolves between the two market configurations.

3.6 Comparative Analysis: 2018 vs. 2025 Datasets

The two datasets represent structurally different European electricity mixes. The 2018 dataset reflects a system still dominated by thermal generation, with relatively flat intra-day price spreads and moderate renewable penetration. The 2025 dataset incorporates a substantially higher share of solar PV across the CWE region, which introduces pronounced intra-day price dynamics and significantly alters both the opportunity for battery arbitrage and the baseline re-dispatch burden. This section compares the two datasets across three dimensions: baseline market conditions, battery cycling behaviour, and the economic outcomes (zonal savings, re-dispatch costs, and net benefit).

3.6.1 Baseline Market Conditions

Zonal price levels

Figure 13 shows the annual average zonal price for each CWE zone under Case 0 (no battery) in both datasets. Prices are systematically lower in 2025 across all zones, reflecting increased renewable generation that depresses the merit-order stack. The Belgian price falls from 55.6 €/MWh in 2018 to 50.5 €/MWh in 2025 (−9.2 %). The most pronounced drop occurs in France (14.8 €/MWh in 2018 vs. 10.6 €/MWh in 2025), consistent with a substantial expansion of wind and solar capacity. Germany/Luxembourg and the Netherlands also see average prices decline by roughly 4–6 €/MWh. Table 21 summarises the baseline zonal prices and the absolute difference between the two datasets.

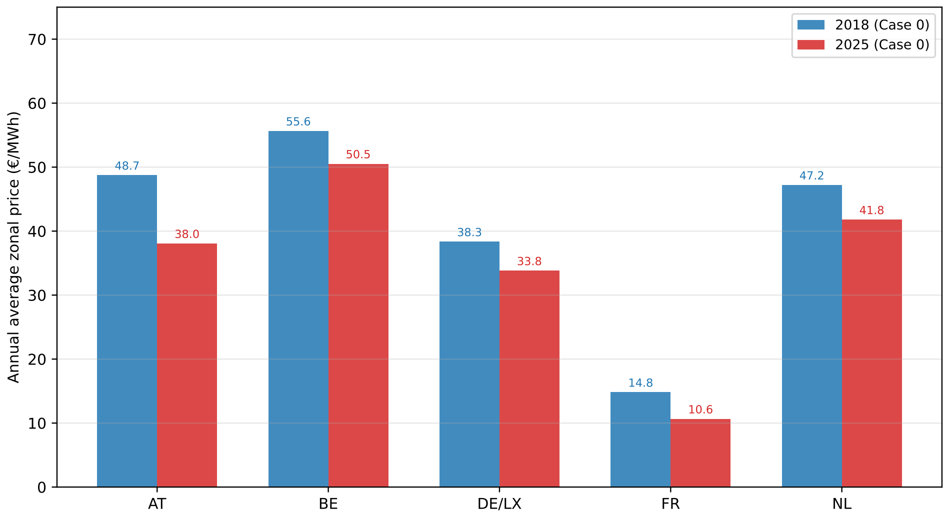

Figure 13: Annual average zonal price (Case 0, no battery) for each CWE zone in 2018 and 2025.

Table 21: Annual average zonal price (Case 0) — 2018 vs. 2025 (€/MWh).

Zone	2018	2025	Difference
AT	48.7	38.0	−10.7
BE	55.6	50.5	−5.1
DE/LX	38.3	33.8	−4.5
FR	14.8	10.6	−4.2
NL	47.2	41.8	−5.4

The particularly low French price in 2025 (10.6 €/MWh, close to the nuclear marginal cost) reflects the structural change in French generation discussed in Section 3.5: with Flamanville 3 online and coal phased out, France's net export volume falls and the marginal unit dispatched sits closer to the nuclear floor.

These price differences have a direct bearing on battery economics. Lower average prices do not necessarily reduce arbitrage value; what matters is the intra-day price spread, which, as shown in the next section, increases markedly in 2025 due to the solar duck curve effect.

3.6.2 Battery Dispatch Patterns

Diurnal cycling profiles

Figure 14 compares the average hourly net battery injection across all cases for the two datasets. The contrast is striking. In 2018, the diurnal profile is relatively flat, with peak discharge amplitudes of roughly 300–400 MW for Case 4 (6,000 MW installed). The price signal is primarily driven by morning and evening demand peaks, but the spread between high and low price hours remains modest.

In 2025, the profile is entirely reshaped by the solar duck curve. From approximately 09:00 to 13:00 UTC, solar generation creates a pronounced price valley, causing batteries to charge at rates exceeding 3,000 MW (Case 4). This is followed by a sharp discharge peak around 18:00–19:00 UTC as solar output falls and evening demand rises. The amplitude of cycling in 2025 is therefore roughly **8 to 10 times larger** than in 2018 for equivalent installed capacity, reflecting the far greater intra-day arbitrage opportunity created by high renewable penetration.

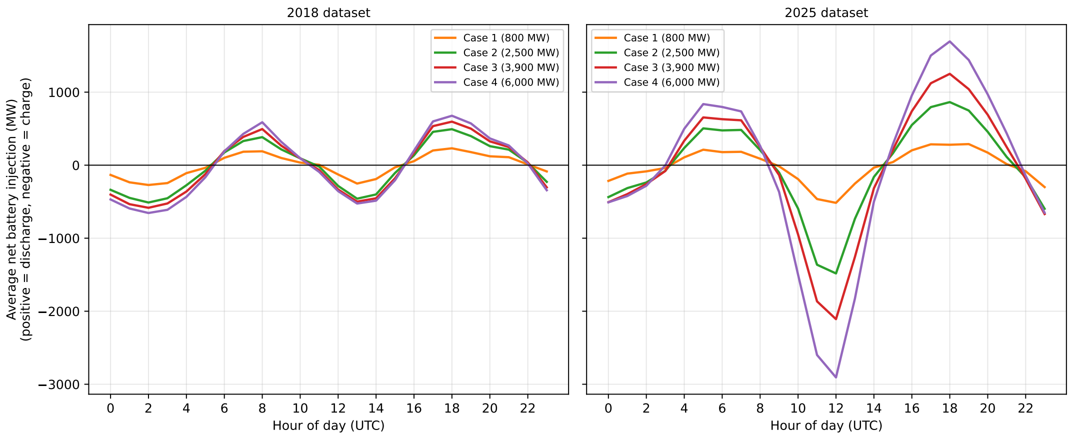

Figure 14: Average net battery injection by hour of day (UTC) for all battery cases, 2018 dataset (left) and 2025 dataset (right). Positive values indicate discharge; negative values indicate charging. The 2025 profile exhibits a pronounced solar duck-curve signature absent in 2018.

This behavioural difference is consequential for system operation: in 2025, large-scale batteries function primarily as daily solar energy shifters, absorbing midday surplus and releasing it during the evening ramp. In 2018, no such structural surplus exists and batteries respond to shallower, less predictable price signals.

3.6.3 Zonal Price Savings and Net Benefit

Belgian generation cost savings

Figure 15 shows, for each battery case, both the Belgian zonal generation cost savings (solid bars) and the net benefit under Method B (hatched bars). Savings are restricted to the hours that are simultaneously feasible under Case 0 and Case k in the re-dispatch model, so that they are directly comparable to the incremental re-dispatch cost ΔC_k^{B}. An important reversal occurs between the two datasets: at small capacity (Case 1, 800 MW), the 2018 dataset yields higher savings (17.0 M€/yr vs. 10.9 M€/yr), because the 2018 price structure offers a more uniform arbitrage opportunity across all hours. As installed capacity increases, the 2025 dataset pulls ahead sharply, reaching 77.6 M€/yr at Case 4 compared to 49.3 M€/yr in 2018. The crossover occurs between Case 2 and Case 3.

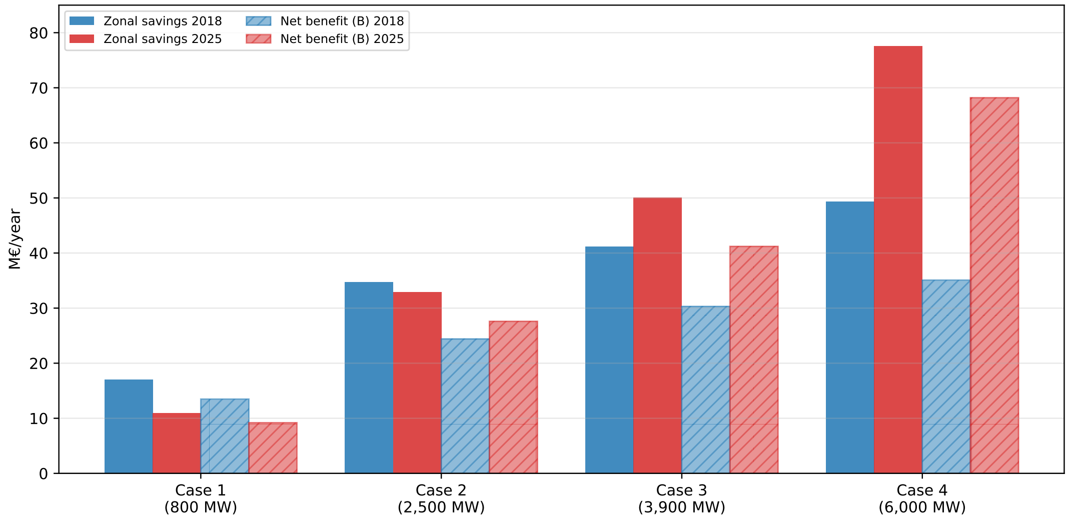

Figure 15: Comparison of Belgian zonal generation cost savings (restricted to re-dispatch-feasible hours) and net benefit under Method B across the four battery cases (2018 vs. 2025). Savings are computed over the intersection of hours feasible under Case 0 and Case k so that they are directly comparable to the incremental re-dispatch cost ΔC_k^{B}.

Net benefit under Method B

The net benefit under Method B (savings minus incremental re-dispatch cost) follows the same crossover pattern. Table 22 summarises all results. At Case 4, the net benefit in 2025 (68.2 M€/yr) is **94 %** higher than in 2018 (35.1 M€/yr), driven by the combination of larger comparable savings and a markedly lower re-dispatch cost increment (+9.4 M€/yr vs. +14.2 M€/yr). Two structural differences between the 2018 and 2025 results deserve attention:

Earlier net benefit crossover than savings crossover: The raw zonal savings only exceed their 2018 level from Case 3 onwards (2025: 50.1 vs. 2018: 41.2 M€/yr); for Cases 1–2 the 2018 scenario still yields higher savings. However, the net benefit crossover occurs one step earlier, between Case 1 and Case 2: at Case 1 the 2018 net benefit (13.5 M€/yr) exceeds the 2025 value (9.2 M€/yr), whereas from Case 2 onwards the 2025 scenario dominates (27.6 vs. 24.4 M€/yr). This earlier crossover reflects the substantially lower incremental re-dispatch costs in 2025 (ΔC_k^{B} = 1.7–9.4 M€/yr) compared with 2018 (3.5–14.2 M€/yr): the 2025 system absorbs additional battery capacity at lower congestion cost, translating savings into net benefit more efficiently.

Widening advantage at large capacity: The gap between the two scenarios grows with battery size. At Case 2 the 2025 advantage is modest (+3.2 M€/yr); by Case 4 it reaches +33.1 M€/yr, a 94 % premium over the 2018 result. This amplification arises because higher renewable penetration in 2025 creates larger intra-day price spreads, so a large battery fleet captures proportionally more arbitrage value while the hard-constraint re-dispatch system benefits from the additional flexibility — a self-reinforcing dynamic that is absent at low battery capacity.

The smaller re-dispatch increment in 2025 (ΔC_B) is explained by the nature of battery operation: in 2025, batteries primarily smooth the midday solar surplus rather than competing with thermal generators for load-following duty, which limits the upward pressure on Belgian generator re-dispatch costs.

Table 22: Belgian zonal savings (comparable hours only), re-dispatch cost increment (Method B), and net benefit — 2018 vs. 2025 (M€/year).

	2018			**2025**		
Case	S_k^{filt}	ΔC_B	Net (B)	S_k^{filt}	ΔC_B	Net (B)
C1 (800 MW)	17.0	3.5	13.5	10.9	1.7	9.2
C2 (2,500 MW)	34.7	10.3	24.4	32.9	5.3	27.6
C3 (3,900 MW)	41.2	10.9	30.3	50.1	8.9	41.2
C4 (6,000 MW)	49.3	14.2	35.1	77.6	9.4	68.2

3.6.4 Re-dispatch Costs

Figure 16 and Table 23 reveal the most structurally significant difference between the two datasets: the level and sign of the Belgian re-dispatch cost.

Under **Method B**, the baseline (Case 0) re-dispatch cost is 222.0 M€/yr in 2018 versus 97.2 M€/yr in 2025 — a reduction of 56 %. This reflects the structural change in the Belgian generation mix: with fewer dispatchable thermal units available in 2025, the scope for costly upward re-dispatch is reduced, keeping C_B lower across all cases. Across all cases the 2025 C_B values remain far below their 2018 counterparts, and the incremental rise with battery deployment is more gradual.

Under **Method A**, the contrast is even more pronounced. In 2018, the CWE-wide re-dispatch optimisation attributes a cost of 356.4 M€/yr to Belgium (Case 0), and this rises to 384.7 M€/yr at Case 4. In 2025, the Belgian share of the CWE-wide re-dispatch cost is **negative** in all cases: −48.2 M€/yr at baseline, reaching −4.7 M€/yr at Case 4. A negative C_A means that, under the CWE-wide optimisation, Belgium acts as a net beneficiary of cross-border re-dispatch flows rather than a net contributor to the cost pool. This sign reversal is a direct consequence of the 2025 generation mix: with large shares of variable renewables, Belgium exports cheap energy during surplus hours, which reduces the overall system cost and credits Belgium accordingly in the CWE-wide allocation.

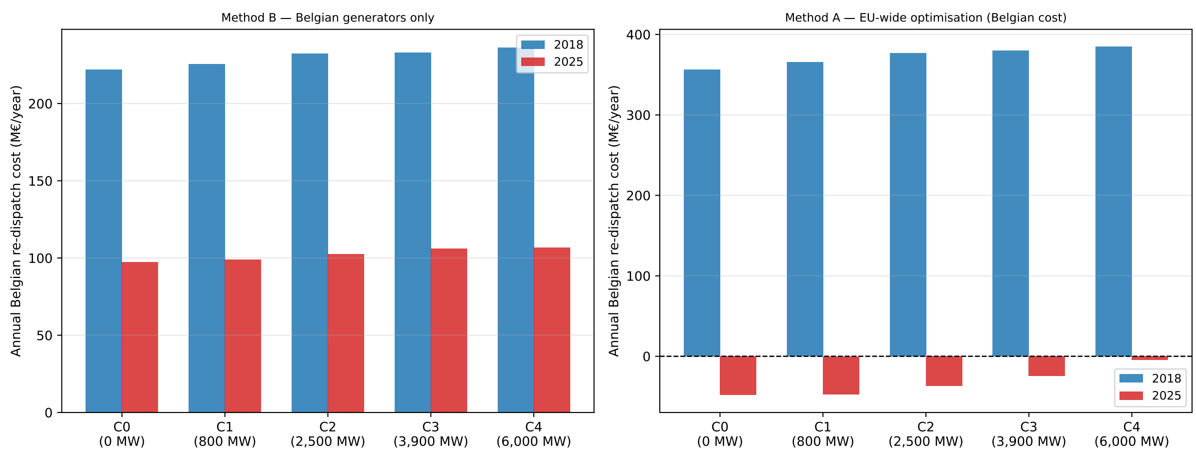

Figure 16: Annual Belgian re-dispatch cost under Method B (left) and Method A (right), for Cases 0–4, comparing the 2018 (blue) and 2025 (red) datasets. Note the sign reversal for Method A in 2025.

It is also notable that in 2025 the Method A cost rises (becomes less negative) as battery capacity increases, from −48.2 to −4.7 M€/yr. This reflects the same mechanism identified in Section 3.5: batteries reduce Belgian price spikes and compress the surplus hours that make Belgium a net beneficiary in the EU allocation, gradually eroding the negative cost advantage.

Table 23: Annual Belgian re-dispatch costs C_B and C_A (M€/year) for all cases — 2018 vs. 2025.

	Method B		**Method A**	
Case	**2018**	**2025**	**2018**	**2025**
C0 (0 MW)	222.0	97.2	356.4	−48.2
C1 (800 MW)	225.5	98.9	365.6	−47.2
C2 (2,500 MW)	232.3	102.5	377.2	−36.7
C3 (3,900 MW)	232.9	106.1	379.9	−24.7
C4 (6,000 MW)	236.2	106.6	384.7	−4.7

3.6.5 Summary of key findings

Table 24 consolidates the main comparison metrics for the largest deployment case (Case 4, 6,000 MW).

Table 24: Summary comparison at Case 4 (6,000 MW) — 2018 vs. 2025.

Metric	**2018**	**2025**
Belgian zonal savings, comp. hours (M€/yr)	49.3	77.6
Re-dispatch cost C_B (M€/yr)	236.2	106.6
Incremental ΔC_B vs. C0 (M€/yr)	14.2	9.4
Net benefit Method B (M€/yr)	35.1	68.2
Re-dispatch cost C_A (M€/yr)	384.7	−4.7
Avg. Belgian price (Case 0, €/MWh)	55.6	50.5
Peak battery cycling amplitude (MW)	≈400	≈3,000

Three conclusions emerge from this comparison. First, the value of large-scale battery storage is **substantially higher** in a high-renewable 2025 system: at 6,000 MW, the net benefit under Method B is 68.2 M€/yr compared to 35.1 M€/yr in 2018, an increase of 94 %. Second, the re-dispatch cost burden is structurally lower in 2025 under both methods, reflecting both lower baseline costs and a smaller marginal cost increment per MW of battery. Third, the Method A sign inversion in 2025 highlights that the choice of re-dispatch accounting methodology has qualitatively different implications depending on the generation mix: in a high-renewable context, Belgium transitions from a net payer to a net beneficiary in the CWE-wide re-dispatch cost allocation, a result with significant policy relevance for the design of cross-border congestion management mechanisms. A fourth finding cuts across both datasets: price-arbitrage BESS is **grid-negative under both market configurations**. In every scenario, under both re-dispatch accounting methods, battery deployment increases rather than decreases Belgian re-dispatch costs. The increment is modest under current TSO practice (Method B): at most 6.4 % of the Case 0 baseline in 2018 and 9.7 % in 2025. Under full EU-wide coordination (Method A), the effect is more disruptive in 2025, where battery charging progressively erodes Belgium's structural re-dispatch credit from −48.2 to −4.7 M€/yr — a loss of 43.5 M€/yr at 6,000 MW. The economic case for large-scale BESS thus rests entirely on the zonal savings exceeding the re-dispatch penalty, not on any congestion-relieving property of storage. Realising the full net benefit will therefore require either a regulatory mechanism that internalises re-dispatch costs into battery dispatch decisions, or a market design that allows TSOs to co-optimise battery schedules with congestion management — a question of growing urgency as Belgian BESS capacity approaches the scales modelled here.

Together, these findings directly answer the thesis's central question: price-arbitrage BESS generates a robustly positive net economic benefit for Belgium under both 2018 and 2025 market conditions, and this benefit grows substantially in a high-renewable system — suggesting that the economic case for large-scale Belgian BESS will strengthen as the energy transition progresses.

4 Limits and Possible Upgrades

The analysis presented in this thesis rests on a set of deliberate modelling choices that allow tractable computation while capturing the essential economics of Belgian BESS in the CWE market. This section identifies the principal limitations of the current framework and outlines the extensions that would most improve its fidelity and scope.

4.1 Limitations

Infeasible hours

Approximately 1,900 hours in 2018 and 2,950–3,011 hours in 2025 (depending on case and method) were flagged as infeasible by the re-dispatch optimisation and excluded from both the annual re-dispatch totals and the zonal savings computation. Restricting savings to the same feasible hours as the re-dispatch costs ensures that the two quantities are compared over an identical set of operating conditions. Since the excluded hours correspond predominantly to extreme winter congestion events, all reported figures constitute lower bounds on the true annual costs. The higher infeasible count in 2025 implies that these lower bounds are proportionally more conservative than in 2018. Importantly, the excluded hours correspond to the most extreme congestion events, where the adverse battery effect would be largest; including them would reinforce rather than reverse the grid-negative conclusion.

Battery dispatch without TSO coordination

Battery schedules are determined entirely by the zonal market optimisation, which has no knowledge of intra-zonal network constraints. The TSO receives fixed battery injection profiles at the re-dispatch stage and must accommodate them rather than co-optimise. This faithfully represents current market arrangements (batteries participate in the day-ahead market as price-takers) but it means the model overstates the re-dispatch cost increase that would arise under a coordinated TSO–BESS dispatch, in which the TSO could, for instance, signal batteries to reduce or shift their charging during congested intervals. A related idealisation is that the zonal model is solved as a single multi-period linear programme over all 8,760 hours, giving batteries perfect annual price foresight. In practice, batteries operate on day-ahead or intraday price forecasts subject to uncertainty; the perfect-foresight assumption overstates both the arbitrage revenue and the cycling intensity relative to what a real operator would achieve.

Zonal representation and method bounds

The zonal market model computes a single clearing price per bidding zone, ignoring intra-zonal price differences. Demand is treated as perfectly inelastic: each zone consumes a fixed quantity regardless of price, so the model captures neither price-responsive demand nor consumer-welfare effects. More broadly, the two re-dispatch accounting methods bracket a range rather than identify a unique cost. Method B leaves CWE-wide violations partially unresolved, while Method A assumes a degree of cross-border TSO coordination that exceeds current practice. The true Belgian re-dispatch cost lies between these bounds, and its precise value depends on the level of TSO coordination actually achieved — a parameter that continues to evolve with European market integration.

Static snapshots and intertemporal constraints

The study relies on two fixed annual datasets and does not model the continuous evolution of the generation mix across intervening years or beyond 2025. An ideally adapted approach would pair each battery scenario with a dedicated generation and load dataset calibrated to the corresponding deployment year (e.g. 2030 or 2035); in practice, forecasting future load profiles and renewable capacity factors introduces substantial uncertainty, so the use of historically observed annual slices is a reasonable trade-off. A second intertemporal gap concerns thermal generator flexibility: minimum up and down times, ramp rates, and nuclear start-up costs are absent from the re-dispatch optimisation. Treating all dispatchable units as fully flexible within their capacity bounds overstates short-run fleet flexibility, particularly for the Belgian nuclear units whose ramping capability is technically limited.

Battery modelling assumptions

All battery scenarios assume a fixed storage duration of 2 hours (energy capacity equal to twice the rated power), consistent with Elia's current CRM contracts. Longer-duration systems (4 h or 8 h) would exhibit deeper daily cycling and different arbitrage profiles, potentially altering both the zonal savings and the re-dispatch impact in ways not captured here. Battery capacity is also distributed across Belgian load buses in fixed proportions derived from the load distribution, without optimising for network impact. Given the PTDF structure of the CWE network, some buses are systematically more exposed to the binding critical branches, and targeted siting could reduce the congestion impact of battery cycling. Optimal placement derived from network sensitivities is left as an avenue for future work.

4.2 Possible Upgrades

Several extensions would directly address the limitations identified above. The highest-priority improvement would be to handle infeasible hours through a penalised relaxation of the re-dispatch problem — introducing load-shedding or curtailment slack variables with high penalty costs — so that extreme events contribute to the annual cost estimates rather than being dropped. This would convert the current lower-bound figures into fuller annual totals and is particularly relevant for assessing battery impact in the high-renewable 2025 context, where infeasible hours are substantially more numerous.

Modelling a coordinated TSO–BESS dispatch, in which battery schedules are jointly optimised with the re-dispatch problem, would quantify how much of the reported re-dispatch cost increase is attributable to the absence of coordination. This extension becomes increasingly important as installed BESS capacity grows: at 6,000 MW, the charging load is large enough to materially shift Belgian intra-zonal flows, and a coordination signal could potentially reduce the net re-dispatch penalty while preserving most of the arbitrage value.

Replacing the zonal market model with a nodal DC-OPF formulation would eliminate the need for a separate re-dispatch stage, provide bus-level locational marginal prices, and allow the BESS siting problem to be solved endogenously. Optimal battery placement could be determined by maximising the reduction in locational price spreads weighted by the PTDF sensitivities of the binding constraints, providing a direct answer to the geographic placement question raised above.

A further modelling upgrade would replace the perfect-foresight annual optimisation with a rolling day-ahead dispatch, in which the battery selects its schedule based only on prices forecast for the next 24–48 hours. This would bring the simulated cycling behaviour closer to real operator practice and provide a lower bound on arbitrage value that, together with the perfect-foresight upper bound reported here, would bracket the range of plausible real-world outcomes. Incorporating demand response — allowing loads to shift or curtail in response to price signals — would complement this extension and lift the perfectly inelastic demand assumption.

Finally, extending the dataset scope to include intermediate projection years — such as 2027 or 2030 — and varying the storage duration assumption across scenarios would allow the relationship between renewable penetration, storage technology, and battery value to be traced as a continuous function rather than captured at two point-in-time snapshots with a single 2-hour design. Coupling this with stochastic renewable generation profiles, rather than the single realised year used here, would provide uncertainty bounds on the reported economic outcomes and strengthen the policy conclusions drawn from the comparative analysis.

5 Conclusion

This thesis set out to answer a concrete question at the intersection of electricity market design and transmission system operation: **does the deployment of battery energy storage in Belgium increase or decrease intra-zonal transmission congestion, and how does this effect evolve as battery capacity scales up?**

To answer it, a two-stage simulation framework was developed and applied to the full Central Western European network under two generation mixes — a 2018 thermal-dominated baseline and an updated 2025 dataset reflecting Belgium's partial nuclear phase-out, the retirement of French and Dutch coal capacity, and the substantial expansion of solar and wind generation across the CWE region. Five battery deployment levels, ranging from zero to 6,000 MW, were evaluated under two re-dispatch accounting methods that bracket the range of plausible TSO coordination.

The results provide a clear and consistent answer to the first part of the question. In both the 2018 and 2025 datasets, and under both accounting methods, battery deployment **increases** Belgian re-dispatch costs relative to the no-battery baseline. The mechanism is structural: batteries optimise their charge-discharge schedule against zonal price signals with no knowledge of intra-zonal network constraints, and the resulting injection and withdrawal patterns impose additional flows on corridors that are already operating near their thermal limits. Charging events tighten the net generation surplus and require the TSO to reduce nearby output; discharge events during peak hours reinforce outbound flows on congested lines and force up-regulation downstream. Both effects raise the cost of restoring network feasibility, and neither is captured by the zonal market clearing. The grid-negative finding is moreover robust to the feasibility filter applied: the excluded hours (approximately 1 900 in 2018 and 2 950–3 011 in 2025) correspond to the most severe winter congestion events, so the reported cost increments are conservative lower bounds on the true annual impact.

The answer to the second part — how the effect evolves — is more nuanced and constitutes the principal scientific contribution of this work. At small capacity (Case 1, 800 MW), the 2018 dataset yields a higher net benefit than 2025 (13.5 M€/yr vs. 9.2 M€/yr), because the more uniform arbitrage opportunities of a thermal-dominated system allow a small fleet to cycle frequently across many hours. As installed capacity increases, the 2025 dataset pulls ahead decisively: at 6,000 MW, the net benefit under Method B reaches 68.2 M€/yr in 2025 versus 35.1 M€/yr in 2018, an increase of 94 %. This crossover reflects the solar duck curve: the pronounced midday price valley created by high photovoltaic penetration concentrates arbitrage value in a small number of hours per day, which a large fleet can exploit far more efficiently than a small one. The amplitude of daily battery cycling in 2025 is roughly 8 to 10 times larger than in 2018 for equivalent installed capacity, and the absolute zonal savings grow correspondingly faster.

The re-dispatch cost increment per unit of battery capacity is, however, *smaller* in 2025 than in 2018. Batteries that absorb midday solar surplus reduce the generation surplus that would otherwise trigger downward regulation of Belgian nuclear units, partially complementing the TSO's congestion management task rather than working against it. The combination of larger savings and a smaller marginal re-dispatch penalty makes the net economic benefit substantially stronger in the high-renewable context for large-scale BESS deployment.

The most structurally significant finding concerns the sign of the Method A re-dispatch cost in 2025. Under the EU-wide optimisation, Belgium's baseline cost is *negative* (−48.2 M€/yr), meaning that Belgian generators are systematically down-regulated to relieve CWE-wide congestion and the associated cost is credited back to Belgium. Battery deployment progressively erodes this credit, reaching −4.7 M€/yr at 6,000 MW. This sign reversal relative to 2018 — when Belgium was a net contributor of 356 M€/yr under Method A — reflects the structural transformation of Belgium's role in the CWE flow regime: from a net provider of congestion relief through upward regulation to a net transit corridor whose cheap nuclear output is curtailed to manage cross-border overloads. The implication is that the economic benefit of large-scale BESS deployment depends critically on the assumed degree of cross-border TSO coordination. Under current practice (Method B), net benefits are robust and growing. Under full EU-wide coordination

(Method A), the erosion of Belgium's re-dispatch credit by large battery fleets raises a genuine policy concern about the distribution of re-dispatch costs across borders as storage capacity continues to scale up.

Taken together, these findings directly address the central research question. Price-arbitrage BESS generates a robustly positive net economic benefit for Belgium under both market configurations and both generation mixes studied. It does so, however, by increasing rather than decreasing intra-zonal re-dispatch costs — a finding that challenges the intuition that flexible storage should relieve network stress. The magnitude of this adverse network effect remains modest relative to the zonal savings (at most 29 % of the benefit under Method B), and it diminishes proportionally as the generation mix shifts toward high renewable penetration. The economic case for large-scale Belgian BESS will therefore strengthen as the energy transition progresses — but realising the full benefit will require either a regulatory framework that internalises the re-dispatch cost externality in battery dispatch, or a market architecture in which TSOs can coordinate storage dispatch across borders without distorting the intra-day price signals that drive arbitrage value in the first place.

References

[1] Anthropic. Claude (claude-sonnet-4-6). https://claude.ai, 2025.

[2] DeepL SE. DeepL translator. https://www.deepl.com, 2025.

[3] Elia. Adequacy and flexibility study for belgium 2026–2036. https://www.elia.be/-/media/project/elia/elia-site/electricity-market-and-system---document-library/adequacy---studies/2025/elia_adequacy_flexibility_study_2026_2036_slides.pdf, June 2025.

[4] Paul Denholm, Erik Ela, Brendan Kirby, and Michael Milligan. The role of energy storage with renewable electricity generation. https://www.nrel.gov/docs/fy10osti/47187.pdf, January 2010.

[5] Bundesnetzagentur and Bundeskartellamt. Monitoring report 2023. https://data.bundesnetzagentur.de/Bundesnetzagentur/SharedDocs/Downloads/EN/Areas/ElectricityGas/CollectionCompanySpecificData/Monitoring/MonitoringReport2023.pdf, November 2023.

[6] Elia. Congestion management costs. https://opendata.elia.be/explore/dataset/ods074/, 2024.

[7] Rahul Walawalkar, Jay Apt, and Rick Mancini. Economics of electric energy storage for energy arbitrage and regulation in New York. https://doi.org/10.1016/j.enpol.2006.09.005, 2007.

[8] Agustín Castillo and Dennice F. Gayme. Grid-scale energy storage applications in renewable energy integration: A survey. https://doi.org/10.1016/j.enconman.2014.07.063, 2014.

[9] Lion Hirth. The market value of variable renewables: The effect of solar and wind power variability on their relative price. https://neon.energy/Hirth-2013-Market-Value-Renewables-Solar-Wind-Power-Variability-Price.pdf, 2013.

[10] Clemens Lohr, Anselm Eicke, and Lion Hirth. Grid utility of large-scale batteries. https://neon.energy/Neon-Netzdienlichkeit-Gro%C3%9Fbatterien-EN.pdf, September 2025.

[11] Anthony Papavasiliou. Optimization models in electricity markets. https://www.cambridge.org/highereducation/books/optimization-models-in-electricity-markets/0D2D36891FB5EB6AAC3A4EFC78A8F1D3#overview, 2022.

[12] Paul Verhagen, Jing Hu, and Robert Harmsen. Evaluating non-firm grid connections for battery energy storage systems: A co-optimization case study of the Netherlands. https://research-portal.uu.nl/ws/portalfiles/portal/273724276/1-s2.0-S0301421525004100-main.pdf, 2026.

[13] Quentin Lêté. Pricing transmission. Lecture slides, LINMA2415: Quantitative Energy Economics, UCLouvain, 2026.

[14] Jeff Bezanson, Alan Edelman, Stefan Karpinski, and Viral B. Shah. Julia: A fresh approach to numerical computing. https://doi.org/10.1137/141000671, 2017.

[15] Miles Lubin, Oscar Dowson, Joaquim Dias Garcia, Joey Huchette, Benoît Legat, and Juan Pablo Vielma. JuMP 1.0: Recent improvements to a modeling language for mathematical optimization. https://doi.org/10.1007/s12532-023-00239-3, 2023.

[16] Julian Hall, Ivet Galabova, Leona Gottwald, and Michael Feldmeier. HiGHS: High performance software for linear optimization. https://doi.org/10.1007/s12532-024-00264-w, 2024.

[17] CEPA. Study on the estimation of the value of lost load of electricity supply in europe. https://www.acer.europa.eu/sites/default/files/documents/en/Electricity/Infrastructure_and_network%20development/Infrastructure/Documents/CEPA%20study%20on%20the%20Value%20of%20Lost%20Load%20in%20the%20electricity%20supply.pdf, July 2018.

[18] Quentin Lété, Yves Smeers, and Anthony Papavasiliou. An analysis of zonal electricity pricing from a long-term perspective. https://doi.org/10.1016/j.eneco.2022.105853, 2022.

[19] ENTSO-E. Actual total load — transparency platform. https://transparency.entsoe.eu/, 2025.

[20] ENTSO-E. Actual generation per production type — transparency platform. https://transparency.entsoe.eu/, 2025.

[21] Bundesministerium für Wirtschaft und Klimaschutz (BMWK). Ministers Lemke and Habeck: Nuclear phase-out makes our country safer. https://www.bmwk.de/Redaktion/EN/Pressemitteilungen/2021/12/20211228-ministers-lemke-and-habeck-nuclear-phase-out-makes-our-country-safer.html, December 2021.

[22] Bundesministerium für Wirtschaft und Klimaschutz (BMWK). Deutschland beendet das Zeitalter der Atomkraft. https://www.bundeswirtschaftsministerium.de/Redaktion/DE/Pressemitteilungen/2023/04/20230413-deutschland-beendet-das-zeitalter-der-atomkraft.html, April 2023.

[23] Chambre des Représentants de Belgique. Projet de loi portant la garantie de la sécurité d'approvisionnement dans le domaine de l'énergie et la réforme du secteur de l'énergie nucléaire. https://www.lachambre.be/FLWB/PDF/55/3852/55K3852001.pdf, April 2024.

[24] ENGIE. Nuclear energy in Belgium. https://corporate.engie.be/en/energy/nuclear-energy, 2025.

[25] EDF. Closure of Fessenheim nuclear power plant. https://www.edf.fr/en/the-edf-group/dedicated-sections/journalists/all-press-releases/closure-of-fessenheim-nuclear-power-plant, 2020.

[26] EDF. Update on the Flamanville EPR: the reactor produces its first electrons on the national electricity grid. https://www.edf.fr/en/the-edf-group/dedicated-sections/journalists/all-press-releases/update-on-the-flamanville-epr-the-reactor-produces-its-first-electrons-on-the-national-electricity-grid, December 2024.

[27] Autorité de Sûreté Nucléaire (ASN). L'ASN autorise la mise en service du réacteur EPR de Flamanville. https://www.asn.fr/l-asn-informe/actualites/l-asn-autorise-la-mise-en-service-du-reacteur-epr-de-flamanville, May 2024.

[28] RTE. Bilan électrique 2024 — rapport complet. https://assets.rte-france.com/prod/public/2025-04/2025-04-09-bilan-electrique-2024-rapport-complet.pdf, 2025.

[29] Ministère de la Transition Écologique et Solidaire. Fermeture des centrales à charbon d'ici 2022 — enjeux et projets de territoire. https://www.ecologie.gouv.fr/sites/default/files/publications/DP_Fermeture%20des%20centrales%20a%20charbon%20d%27ici%202022%20-%20Enjeux%20et%20projets%20de%20territoire.pdf, January 2020.

[30] Eerste Kamer der Staten-Generaal. Wet verbod op kolen bij elektriciteitsproductie (35.167). https://www.eerstekamer.nl/wetsvoorstel/35167_wet_verbod_op_kolen_bij, 2019.

[31] Vattenfall. Vattenfall's last coal power plant in the Netherlands is closing. https://group.vattenfall.com/press-and-media/newsroom/2019/vattenfalls-last-coal-power-plant-in-the-netherlands-is-closing/, December 2019.

[32] RWE. Amercentrale — biomass-fired power plant. https://benelux.rwe.com/en/locations-and-projects/amer-power-plant/, 2025.

[33] Elia. Elia and Amprion launch ALEGrO, the first interconnector between Belgium and Germany. https://www.elia.be/-/media/project/elia/shared/documents/press-releases/2020/20201109_cp-alegro-inauguration_en.pdf, November 2020.

[34] Amprion. ALEGrO — first anniversary of the Belgium–Germany interconnector. https://www.amprion.net/Press/Press-Detail-Page_37505.html, 2020.

[35] Stefan Pfenninger and Iain Staffell. Renewables.ninja. https://www.renewables.ninja/, 2025.

[36] Stefan Pfenninger and Iain Staffell. Long-term patterns of European PV output using 30 years of validated hourly reanalysis and satellite data. https://doi.org/10.1016/j.energy.2016.08.060, 2016.

[37] Centraal Bureau voor de Statistiek (CBS). Renewable electricity: Production and capacity. https://www.cbs.nl/en-gb/figures/detail/82610ENG, 2025.

UNIVERSITÉ CATHOLIQUE DE LOUVAIN
École polytechnique de Louvain
Rue Archimède, 1 bte L6.11.01, 1348 Louvain-la-Neuve, Belgique | **www.uclouvain.be/epl**